

**THIS BOOK IS OF
POOR LEGIBILITY
DUE TO LIGHT
PRINTING
THROUGH OUT IT'S
ENTIRETY.**

**THIS IS AS
RECEIVED FROM
THE CUSTOMER.**

SEPARATION AND PURIFICATION OF THE SOLID SOLUTION SYSTEM
INDOLE-INDENE BY CONTINUOUS COUNTERCURRENT COLUMNAR CRYSTALLIZATION

by

ALBERT TZE-HSUAN LIN

B.S. National Taiwan University, 1961

42-6074

A MASTER'S THESIS

submitted in partial fulfillment of the

requirements for the degree

MASTER OF SCIENCE

Department of Nuclear Engineering

KANSAS STATE UNIVERSITY
Manhattan, Kansas

1972

Approved by :


Major Professor

**THIS BOOK
CONTAINS
NUMEROUS PAGES
WITH THE ORIGINAL
PRINTING BEING
SKEWED
DIFFERENTLY FROM
THE TOP OF THE
PAGE TO THE
BOTTOM.**

**THIS IS AS RECEIVED
FROM THE
CUSTOMER.**

LD
2668
74
1972
L54
C.2
Docu-
ment

CONTENTS

1.0	INTRODUCTION	1
2.0	LITERATURE REVIEW	3
3.0	THEORY	10
3.1	Review of Mathematical Models	10
3.2	The Mass and Energy Continuity Equations	12
3.3	Mass Transfer Limiting with Latent Heat Effect Model	15
3.4	Mass Transfer Limiting Model	17
4.0	EXPERIMENTAL STUDY	23
4.1	Equipment Description	23
4.2	Data Measurement Procedure	26
4.3	Choice of System	27
4.4	Quantitative Analysis of Column Sample	27
5.0	EXPERIMENTAL RESULTS AND DISCUSSIONS	31
5.1	Experimental Results	31
5.2	Test of Experimental Column Performance with the Mass Transfer Limiting with Latent Heat Effect Model	31
5.3	Test of Experimental Column Performance with the Mass Transfer Limiting Model	43
5.4	Effect of Reflux Ratio on Free Liquid Concentration Profile	48
6.0	CONCLUSIONS	54
7.0	ACKNOWLEDGEMENTS	56
8.0	REFERENCES	57
9.0	APPENDICES	60
	Appendix A: Physical Properties of Indole-Indene System	61
	Appendix B: Phase Equilibrium Data of Indole-Indene System	63

Appendix C: Estimation of Heat Capacity of Liquids by the Additivity Rules	64
Appendix D: Method for the Estimation of the Latent Heat of Fusion	68

LIST OF FIGURES

1. Diagram of Schildknecht-Type Column Crystallizer as Described by Gates, Albertins and Powers	5
2. Diagram of Center-Fed Schildknecht-Type Column Crystallizer as Described by Gates, Albertins and Powers	6
3. Philips Piston-Type Column as Described by Player	7
4. Philips Pulsed-Type Column as Described by Player	8
5. Diagram Illustrating Solid and Liquid Phase Relationship in Columnar Crystallization Process	13
6. Differential Element in Purification Section of Column Crystallizer	18
7. Countercurrent Continuous Crystallization Separation and Purification System	24
8. Solids and Liquid Pumping Action of Pulse-Check Valve Combination	25
9. Indole-Indane Phase Diagram	28
10. Calibration of Standard Sample Radioactivity	30
11. Free Liquid Concentration Profile of Data Set 1A and 1C	32
12. Free Liquid Concentration Profile of Data Set 1B and 1D	33
13. Free Liquid Concentration Profile of Data Set 2A and 2C	34
14. Free Liquid Concentration Profile of Data Set 2B and 2D	35
15. Free Liquid Concentration Profile of Data Set 3A and 3C	36
16. Free Liquid Concentration Profile of Data Set 3B and 3D	37
17. $\ln\left(\frac{y - y_f}{y_o - y_f}\right)$ vs. Z Modified Free Liquid Concentration Profile of Data Set 1A	39
18. $\ln\left(\frac{y - y_f}{y_o - y_f}\right)$ vs. Z Modified Free Liquid Concentration Profile of Data Set 2A	40
19. $\ln\left(\frac{y - y_f}{y_o - y_f}\right)$ vs. Z Modified Free Liquid Concentration Profile of Data Set 3A	41

20.	Examination of Parameter A of the Mass Transfer Limiting with Latent Heat Effect Model	42
21.	Determination of the Parameter H of the Mass Transfer Limiting Model	44
22.	Determination of Diffusivity and Mass Transfer Coefficient for Indole-Indene by Using the Mass Transfer Limiting Model	46
23.	Effect of Crystal Flow Rate on Separating Ability. Comparison of Experimental and Calculated Values of H for the System Indole-Indene	47
24.	Qualitative Illustration of the Relation between A/V and Free Liquid Reflux Rate	52
25.	Qualitative Illustration of the Relation between Void Fraction and Free Liquid Reflux Rate	53

LIST OF TABLES

I. Values of Effective Diffusivity, Mass Transfer Coefficient and Void Fraction	20
II. Influence of Difference in Phase Compositions on Separation	49
III. Group Values Used to Calculate Constant-Pressure Heat Capacity of Liquids at 25°C and 1 atm. Cal, mole ⁻¹ , deg. ⁻¹	66

NOMENCLATURE

- A = constant defined by equation (12), cm^{-1}
 a = interfacial area, cm^2/cm^3 of packed bed
 b = intercept of phase relation, equations (7) and (16), weight fraction
 C = constant in general solution to differential equation (19), weight fraction
 C_p = specific heat, $\text{Cal/g} \cdot ^\circ\text{C}$
 D = effective axial diffusivity, cm^2/sec
 H = grouping of variables defined by equation (28), cm
 h = total column length, cm ; heat transfer coefficient, $\text{cal/sec}, \text{cm}^2, ^\circ\text{C}$
 K = mass transfer coefficient, cm/sec
 L = solid phase flow rate, $\text{g/sec}, \text{cm}^2$
 m = slope of phase relation, equations (7) and (16)
 N = diffusional flow of material, $\text{g/cm}^2, \text{sec}$
 q = constant defined by equation (20)
 R = reflux ratio; constant defined by equations (17)
 T = temperature, $^\circ\text{C}$
 V = free liquid flow rate, $\text{g/sec}, \text{cm}^2$
 X = high melting component in solid solutions, weight fraction
 y = high melting component in the free liquid, weight fraction
 z = location in column above bottom, cm
 ϵ = void fraction, dimensionless
 ρ = chemical system density, g/cm^3
 λ = total heat of solution, cal/g

SUBSCRIPTS

- f = initial occluded liquid condition
 s = solid surface condition

1.0 INTRODUCTION

Beginning in 1965 at Kansas State University, a study of the application of fractional crystallization to the separation and purification of materials was initiated with the long range objective of applying the knowledge gained to the separation and purification of nuclear fuels and materials.

Separation and purification by crystallization is based on the phase equilibria between solid and liquid. In general two types of equilibria exist, solid-insoluble eutectic type and solid-solution type. Independent of the type of equilibria, the fractional crystallization-purification process has been considered to depend on the growth and dissolution of crystals.

In the earlier studies by Meyer and Shen^{11,12}, emphasis was placed on determining which transport properties would significantly affect the separation of materials by continuous countercurrent crystallization. Meyer and Shen, not being able to include the high temperature and costly sophisticated equipment that would be required for work with nuclear fuels and materials, studied the organic solid-insoluble eutectic systems benzene-naphthalene and p-xylene-m-xylene. In this earlier work countercurrent crystallization equipment was developed as were experimental techniques and procedures. From their studies of the solid-insoluble eutectic system experimental concentration and temperature profiles for the free liquid, Meyer and Shen suggested that a mass transfer limiting with latent heat effect mathematical model was suitable for correlating the purification process data.

As noted by Powers²³, Gates⁶, and Meyer and Shen^{11,12}, the behavior of crystals formed from chemical mixtures of the solid-insoluble eutectic

type and the solid solution type would be different. Thus the mathematical models which are applicable in correlating the performance of solid-insoluble eutectic systems and solid solution systems would probably be different. Meyer and Shen expected that the mass transfer limiting model would govern the separation processes for solid-solution systems, and they suggested further studies of solid-solution systems to confirm or invalidate this conclusion. The study reported in this thesis was undertaken with this purpose. The goal was to test which mathematical model is suitable in correlating the performance of solid-solution systems in column purification processes.

In this study, the mathematical models chosen to be tested were the mass transfer limiting with latent heat effect model developed by Meyer and Shen^{11,12}, and the mass transfer limiting model developed by Gates⁶. The reasons for limiting mathematical models to these two include: first, they are the latest developed; second, they are proved experimentally with confidence by the authors; and third, both are regarded by the authors as applicable to both solid-insoluble eutectic systems and solid solution systems.

In this study, a low melting organic solid-solution system indole-indene was chosen because of the temperature limitations of the available equipment and the fact that the phase equilibrium data were available for this system.

2.0 LITERATURE REVIEW

Separation by crystallization has been used by man to improve his living standard for thousands of years. Before written records, crystallization was used to separate salt from sea water. Conventional crystallization processes were all batch operations, multiple step batch crystallization with recombination of fractions of about the same melting point were used for difficult separations. One of the reasons for this development was the batchwise equipment required to separate crystals from the occluded mother liquor.

A countercurrent continuous fractional crystallization process analogous to continuous fractional distillation was first patented by P. M. Arnold²² in 1951.

Crystallization has two advantages over distillation and solvent extraction as a separation method: Heats of fusion are much lower than heats of vaporization and for solid-insoluble eutectic systems only one theoretical stage is required for separating a 100% pure component from a binary mixture, no other separation process offers this possibility, even in theory.

Subsequent to Arnold's patent, two significant different modifications of column crystallization have evolved. The first one deriving from the patent of Arnold is called the Philips column crystallizer; this device is primarily used in the industrial scale production of materials. The other type of crystallizer is that developed by Schildknecht; it is used in the laboratory to produce materials of high purity.

An analysis of separation and purification in a Schildknecht crystallization column (Figures 1 and 2) of both eutectic and solid-solution systems by the theory of differential countercurrent contacting has been

discussed by Powers²³. The operation variable considered were feed rate and rate of crystal formation, as well as speed, frequency, and amplitude of spiral rotation. This work was continued by Henry⁷, Albertins¹, and Gates⁶. Efforts have been made by these workers to develop mathematical models to predict the performance of crystallization columns. The resulting mass transfer limiting models for both eutectic and solid-solution systems contain undetermined column parameters which can only be evaluated from experimental data. The energy transfer and latent heat effects related to the interfacial mass transfer were not considered in the development of these models.

References to the Philips column by Weedman, and McKay^{9,10,24} have dealt with improvements in its operation and control. This process has been applied to the system p-xylene--m-xylene to recover p-xylene of high purity (99.5%) by both piston type (Figure 3) and pulse type (Figure 4) columns. The controlling factor determining product purity is the temperature of the liquid in the melting zone. The other process variables are feed composition, rate of removal of mother liquor by filtration, control of the crystal phase movement, and heat transfer in the melting section. The capability of scaling-up pilot plant size columns to commercial size has been reported. The column can be used for separating many other chemical systems than those for which it is now commercially applied. However, the purification mechanisms controlling the continuous crystallization process and the mass transfer characteristics have not been elucidated fully by that work.

A mathematical analysis of the separation of a eutectic system, p-xylene--m-xylene, based on the end-fed Philips column has been presented by Player¹⁴. The calculations were based on the total mass and heat balance

**THIS BOOK
CONTAINS
NUMEROUS PAGES
WITH DIAGRAMS
THAT ARE CROOKED
COMPARED TO THE
REST OF THE
INFORMATION ON
THE PAGE.**

**THIS IS AS
RECEIVED FROM
CUSTOMER.**

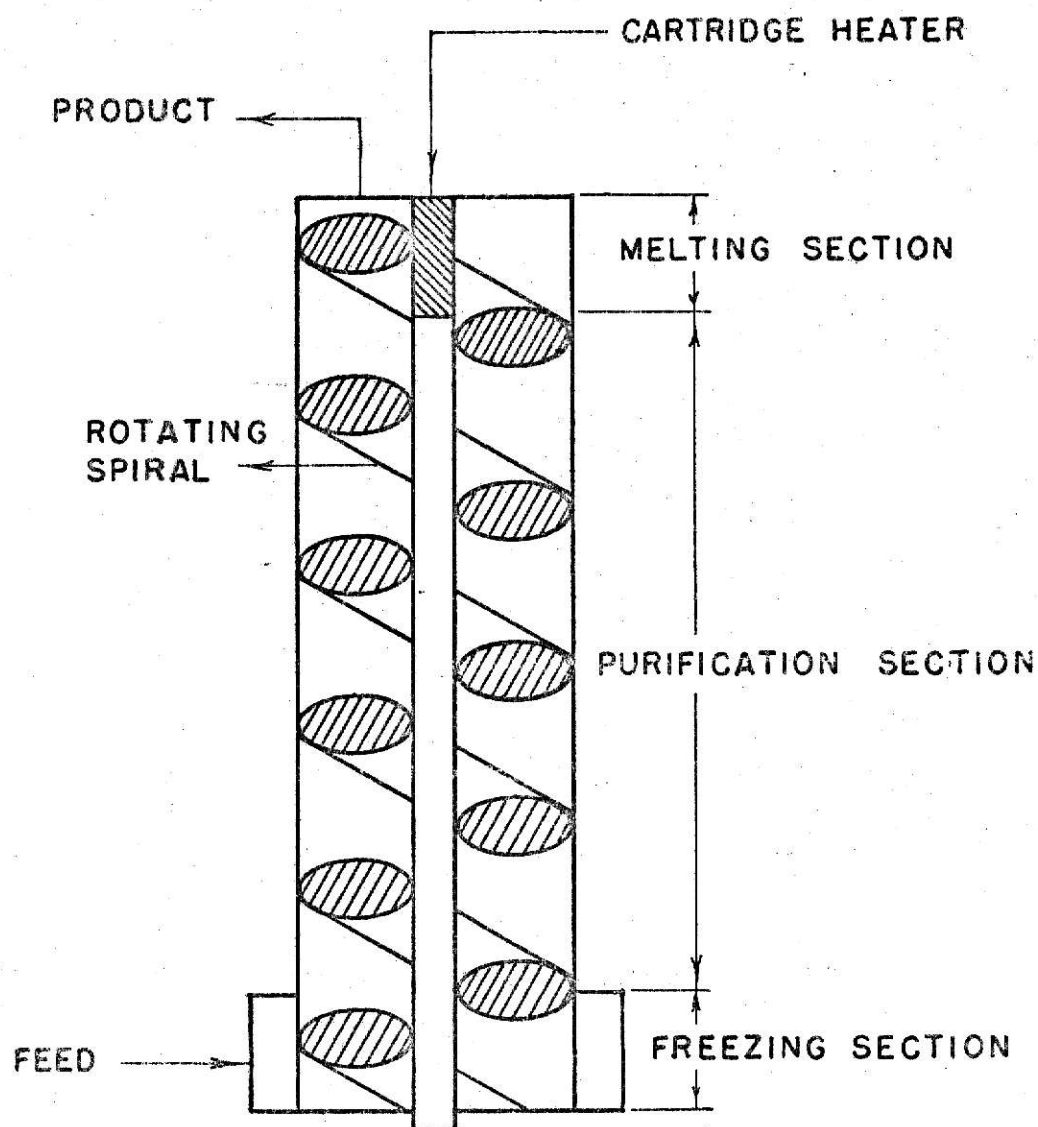


FIGURE 1: DIAGRAM OF SCHILDKNECHT - TYPE COLUMN CRYSTALLIZER AS DESCRIBED BY GATES, ALBERTINS AND POWERS ^{6, 1, 23}

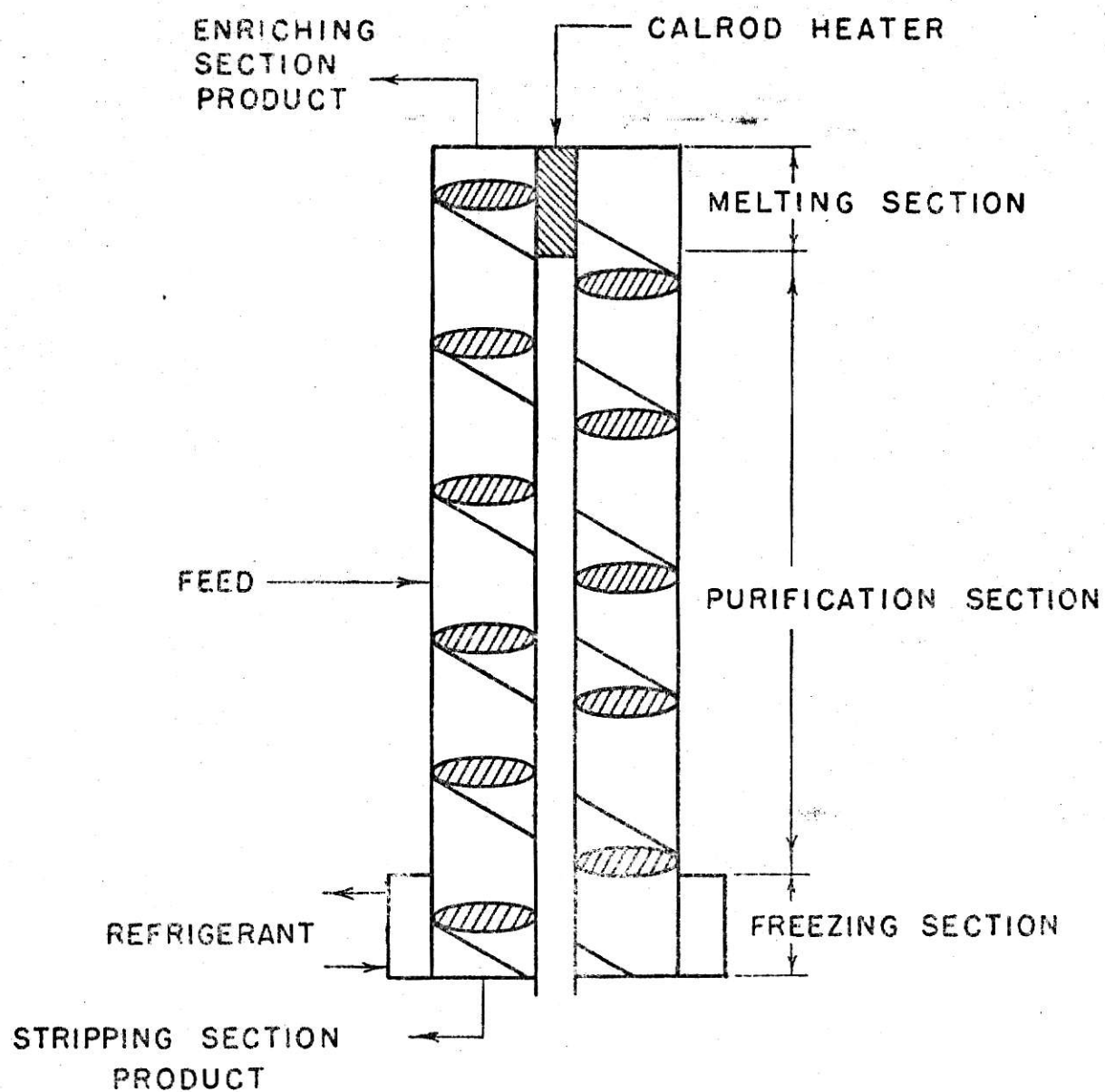


FIGURE 2: DIAGRAM OF CENTER-FED SCHILDKNECHT TYPE COLUMN CRYSTALLIZER AS DESCRIBED BY HENRY ⁷

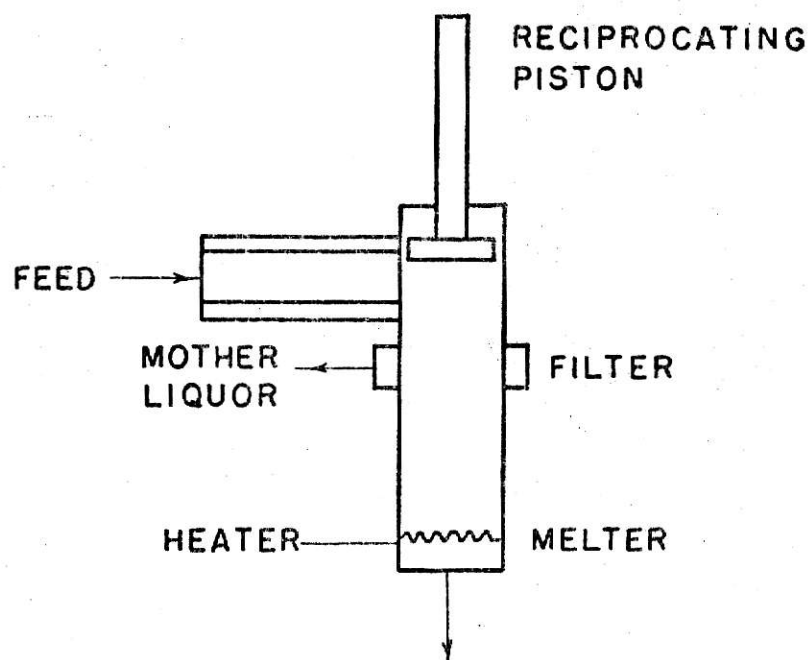


FIGURE 3: PHILIPS PISTON-TYPE COLUMN
AS DESCRIBED BY PLAYER ¹⁴

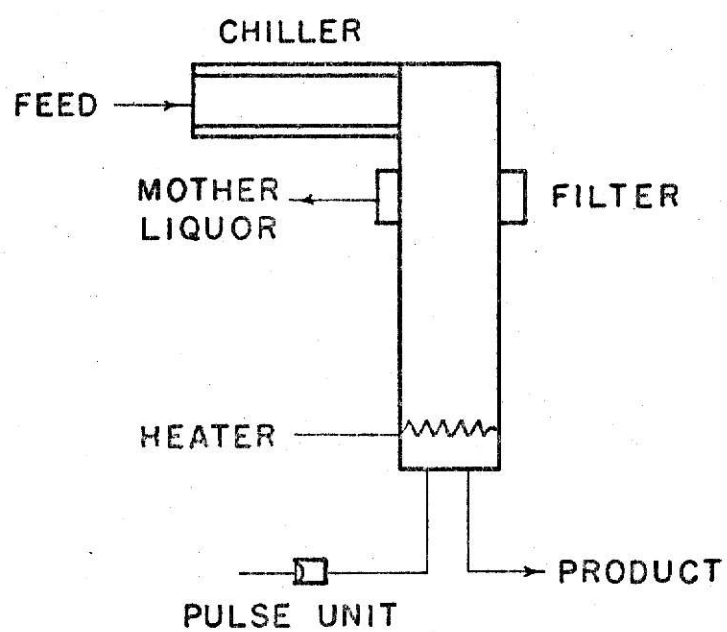


FIGURE 4: PHILIPS PULSED - TYPE COLUMN
AS DESCRIBED BY PLAYER 14

between solid and reflux streams. Both calculation and experimental data showed a sharp change in concentration and temperature profiles at the interface of the purification and compaction zones. These results indicated the importance of recrystallization of the reflux liquid and thermal equilibrium in the solid and liquid phases as limiting factors in the column purification process.

Separation and purification in an end-fed crystallization column by the theory of differential countercurrent contacting have been discussed by Meyer and Shen^{11,12}. Eutectic systems naphthalene-benzene and p-xylene--m-xylene were used in experimental studies. The operation variables considered were solid phase mass flow rate and the rate of heat input at the melting zone. A mass transfer limiting with latent heat effect mathematical model was developed to predict the performance of crystallization columns. The experimental results showed that the stable range of operation and the extent of purification are limited by the rate of thermal equilibrium in the melting zone at the bottom of the purification column.

3.0 THEORY

3.1 Review of Mathematical Models

Two mathematical models applicable to column crystallization based on the theory of differential countercurrent contacting were chosen to be tested in this study. They are the mass transfer limiting with latent heat effect model developed by Meyer and Shen^{11,12}, and the mass transfer limiting model developed by Gates⁶.

In the development of these two models the following assumptions are common: (1) the occluded liquid is in equilibrium with the pure crystalline phase, (2) the composition within each phase is uniform in the plane perpendicular to flow, (3) the free liquid rising in the column is at its freezing point, (4) effective diffusivity D , mass transfer coefficient Ka , the column cross section area A , and the volume fraction of the column occupied by liquid ϵ , as well as the liquid and solid mass flow rates V and L , are independent of position in the column.

Examination of a binary mixture indicates that the high melting component will concentrate in the melting section. Thus as a crystal moves toward this section, it moves into a region of increasingly high temperature and composition of the high melting component. As the solid phase, which is a composite of crystals and occluded mother liquor, is completely melted in the melting section, a part of the melt will be drawn off as bottom product, and the rest of the melt will be refluxed back up the column as the free liquid. The free liquid will pass into a region of lower temperature and lower concentration in the occluded liquid. The temperature and concentration differences between the upward flowing free liquid and downward flowing solid stream may lead to a simultaneous transfer of both heat and mass between

the streams. The descending solid phase is heated and becomes unstable. This instability must be relieved by a change in composition. The probable process will be melting of a portion of the crystals by the absorbed energy; followed by the formation of new crystals and mother liquor purer in high melting component.

The different authors considered the same mechanisms to be involved in the development of these two models for column crystallization^{6,11,12}. However, they treated the problem using different analytical procedures. Gates reasoned that the inclusion of both mass and heat transfer coefficients in a general mathematical description would be too complex. Consequently, he split the problem into two simplified cases. In the first simplified model, he assumed that the heat transfer coefficient was large and that the rate of mass transfer thus is limited by a mass transfer coefficient. This analysis resulted in the mass transfer limiting model. In the second, it was assumed that the mass transfer coefficient was large and that the interphase transfer was restricted by a heat transfer coefficient. This results in the heat transfer limiting model. Finally he concluded that of the two models the mass transfer limiting model was in agreement with his experimental results.

The mass transfer limiting model assumes the changes in composition which occur in the solid phase as it passes toward the melting section are limited (controlled) by the rate at which mass transfer can occur, and that neither intraphase diffusion nor interphase heat transfer control the observed effects. Thus the resulting mass transfer limiting model is simplified by neglecting heat transfer effects. In the case of a solid solution

system. Gates concluded that the mass transfer limiting model leads to the prediction of a linear composition profile.

Meyer and Shen^{11,12} assumed that heat transfer was a much faster process than mass transfer in column crystallization. However, they considered that the heat transfer, in addition to mass transfer, may be a limiting or rate controlling process. Heat transfer between the free liquid and solid streams includes a latent and sensible heat energy exchange. They found experimentally that the interfacial heat transfer coefficient, which is in connection with the sensible heat energy exchange between free liquid and solid streams, was limited to a theoretical maximum value on the order of 10^{-4} cal/cm², sec °C. Thus they concluded that the interfacial heat transfer was negligible compared to the latent heat effect. The resulting mass transfer limiting with latent heat effect model is simply the coupling of mass and energy continuity equations but neglecting the interfacial heat transfer.

3.2 Mass and Energy Continuity Equations

A diagram illustrating solid and liquid phases relationships in columnar crystallization processes are shown in Figure 5. The transport of matter through a fluid flowing in a porous medium may depend on both molecular diffusion and mixing of different portions of the fluid caused by their dissimilar relative motions. The vertical motion of eddies within the body of the fluid may physically transport dissolved solute in bulk. This mixing is generally called eddy diffusion and is treated in terms of a diffusivity in a manner analogous to Fick's first law for molecular diffusion. According to Fick's first law of diffusion⁵, the total axial dispersion of high melting component at z is written as:

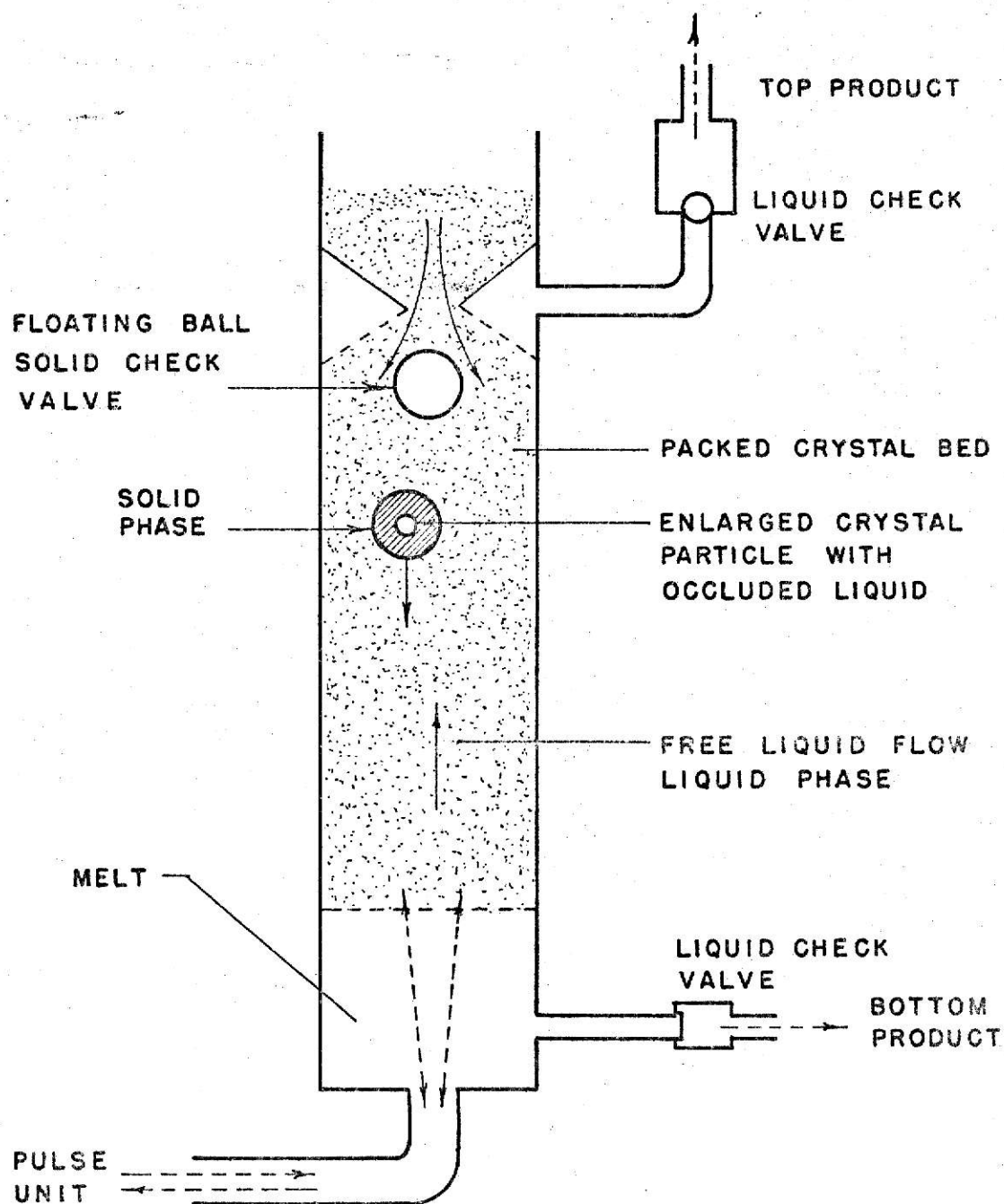


FIGURE 5: DIAGRAM ILLUSTRATING SOLID AND LIQUID PHASES RELATIONSHIP IN COLUMNAR CRYSTALLIZATION PROCESS

$$N_A = y(N_A + N_B) - \rho \epsilon D \frac{dy}{dz} . \quad (1)$$

In the radial direction, material transfers from the solid to the liquid phase primarily as a result of melting and refreezing. The mass transfer is assumed to be proportional to a mass transfer coefficient Ka and to the displacement from equilibrium between phase $(y - y_s)$. From the shell balance of high melting components, the net leakage rate in the z direction is:

$$\frac{dN_A}{dz} = -\rho Ka(y - y_s) . \quad (2)$$

Substitute equation (1) into equation (2). If the temperature gradient along the column is small, the free liquid density, ρ , can be assumed to be independent of column height z . The mass continuity equation can then be written as:

$$\rho \epsilon D \frac{d^2 y}{dz^2} - V \frac{dy}{dz} - Ka \rho (y - y_s) = 0 . \quad (3)$$

The transfer of mass also represents a transfer of energy between solid and liquid phases. The total change in enthalpy of the free liquid will be due to a latent and sensible heat energy exchange with the descending composite solid stream. The loss of heat energy by the rising free liquid can be described in terms of a simultaneous exchange of heat and mass between the two passing streams. If viscous dissipation heat of mixing and axial heat conduction in the liquid phase are neglected, the differential heat balance can be derived similarly for the high melting component in the free liquid as:

$$C_p V \frac{dT}{dz} + ha(T - T_s) + \rho \lambda Ka(y - y_s) = 0 . \quad (4)$$

3.3 Mass Transfer Limiting With Latent Heat Effect Model

The mass transfer limiting with latent heat effect model is the result of the coupling of mass and energy continuity equations, but neglecting the interfacial heat transfer. Meyer and Shen^{11,12} observed that the degree of mixing of the solid and liquid phases does not change the measured free liquid concentration profiles. They also found that the calculated maximum interfacial heat transfer coefficient is negligibly small compared to the latent heat effect. Based on these facts, they concluded that the interfacial heat transfer does not act as a limiting factor in the purification process. The differential heat balance equation (4) is then reduced to the following expression,

$$C_p V \frac{dT}{dz} + \rho \lambda K_a (y - y_s) = 0 \quad . \quad (5)$$

The resulting differential equation obtained by the coupling of the mass and energy continuity equations is free from the solid phase variables as noted below

$$\frac{d^2 y}{dz^2} - \frac{V}{\rho \epsilon D} \frac{dy}{dz} + \frac{C_p V}{\lambda \rho \epsilon D} \frac{dT}{dz} = 0 \quad . \quad (6)$$

Equation (6) which describes the mass transfer limiting with latent heat effect model contains two variables, y (free liquid concentration) and T (free liquid temperature). The problem would be simplified if these two variables were not independent of each other.

The assumption that the free liquid is always saturated has been mentioned. Therefore, it is assumed that y 's and T 's are related by the solubility data for the system being separated. Generally the solubility function is approximately linear (particularly over a narrow concentration range); therefore, y can be expressed as a linear equation in T :

$$y = b_1 + m_1 T \quad (7)$$

Thus equation (6) can be reduced to a one variable second order linear differential equation:

$$\frac{d^2 y}{dz^2} + \frac{V}{\rho \epsilon D} \left(\frac{C_P}{\lambda m_1} - 1 \right) \frac{dy}{dz} = 0 \quad (8)$$

The boundary conditions are:

$$y = y_o \quad \text{at} \quad z = 0 \quad (9)$$

$$y = y_f \quad \text{at} \quad z \rightarrow \infty \quad (10)$$

Meyer and Shen^{11,12} assumed, as shown in equation (10), that the free liquid concentration at the top of a sufficiently long column ($z = \infty$) should approach the initial occluded liquid concentration, y_f , where the concentration gradients in both the axial direction and interfacial film have vanished. Thus y_f is dependent on the feed concentration and freezing temperature according to the phase diagram of the system being separated.

The solution of equation (8) which describes the free liquid concentration in the liquid phase is:

$$y = y_f + (y_o - y_f)e^{-Az} \quad (11)$$

where

$$A = \frac{V}{\rho \epsilon D} \left(\frac{C_P}{\lambda m_1} - 1 \right) \quad (12)$$

The mass transfer limiting with latent heat effect model thus predicts an exponential free liquid concentration profile. A plot of the experimental data in the form of $\ln\left(\frac{y - y_f}{y_o - y_f}\right)$ vs. z should be a straight line with slope $(-A)$. It has been shown above that the results are independent of solid phase variables; thus the model may be applied to both solid-insoluble eutectic and solid-solution systems.

From the experimentally measured slope $(-A)$, the effective axial diffusivity can be evaluated from the following equation:

$$D = \frac{V}{\epsilon \rho A} \left(\frac{C_P}{\lambda m_1} - 1 \right) \quad (13)$$

3.4 Mass Transfer Limiting Model

The basic equation, describing the physical phenomena, is a differential mass balance equation in a differential volume of the column analogous to equation (3) derived in the previous section. To solve this equation the occluded liquid concentration, y_s , must be eliminated or expressed in terms of system physical constants and variables. This is done by total mass balance and end point mass balance (Figure 6) of high melting component in all flows, i.e., solid crystal, occluded liquid, and free liquid streams. For a column operating at total reflux

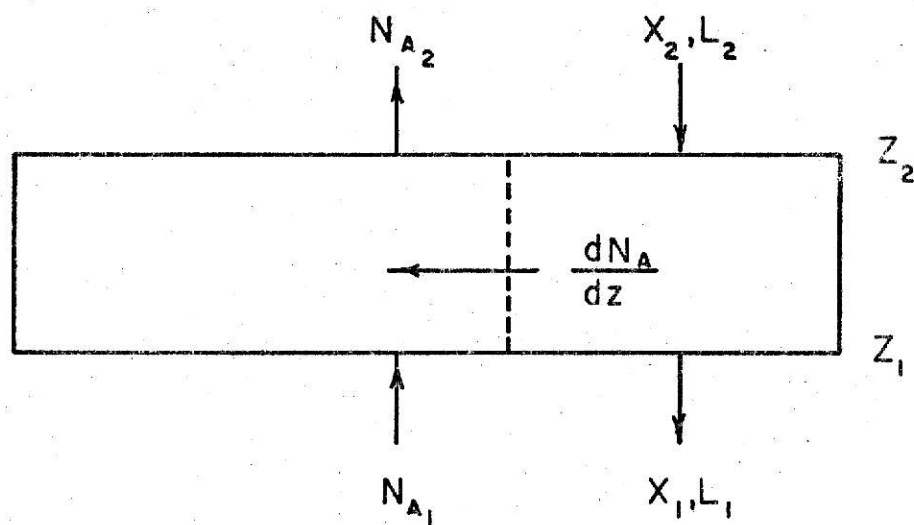
$$\rho \epsilon D \frac{d^2 y}{dz^2} - V \frac{dy}{dz} - K a \rho (y - y_s) = 0 \quad (3)$$

$$L - V = 0 \quad (14)$$

$$\epsilon \rho D \frac{dy}{dz} + LX - VY = 0 \quad (15)$$

The solution of equations (3), (14) and (15) requires another relationship between the dependent variables. Solid-liquid phase equilibrium data serve to relate y_s and X . In general, the phase equilibrium relation is a linear function over a reasonable range of compositions (particularly for a solid solution system which has a small separation factor). Therefore

$$X = b_2 + m_2 y_s \quad (16)$$



$$N_A = y (N_A + N_B) - \rho \epsilon D \frac{dy}{dz}$$

FIGURE 6 DIFFERENTIAL ELEMENT IN PURIFICATION SECTION
OF COLUMN CRYSTALLIZER

Values for b_2 and m_2 can be determined for the range of composition which applies in a given separation. Combining equations (3) and (14) through (16), and introducing the definitions given by equations (17), one obtains a differential equation describing the concentration profile achieved in a column crystallization process involving a solid solution system is

$$R_1 \equiv \frac{L}{\epsilon D \rho} + \frac{K a \rho}{L m_2} \quad (17a)$$

$$R_2 \equiv \frac{K a}{D \epsilon} \left(1 - \frac{1}{m_2}\right) \quad (17b)$$

$$\frac{d^2 y}{dz^2} - R_1 \frac{dy}{dz} - R_2 \left(y + \frac{b_2}{m_2 - 1}\right) = 0 \quad (18)$$

The solution to equation (18) has the form:

$$y = -\frac{b_2}{m_2 - 1} + C_1 \exp(q_1 z) + C_2 \exp(q_2 z) \quad (19)$$

The constants q_1 and q_2 must satisfy the characteristic equation:

$$q^2 - R_1 q - R_2 = 0 \quad (20)$$

Approximate values of the groupings R_1 and R_2 can be obtained by estimating values of the parameters comprising the groups. Values of m_2 and ρ are obtained from physical data on the system being investigated. Values of D and Ka can be approximated from data on liquid extraction in pulsed columns, and reasonable values of ϵ have been reported (see Table 1). By applying such estimated values it has been established that the particular grouping $4R_2/R_1^2$ was less than 0.1 for all runs made in the course of this investigation. Under these conditions, the roots of equation (20) can be closely approximated as:

$$q_1 = R_1 \quad (21)$$

$$q_2 = -\frac{R_2}{R_1} \quad (22)$$

Table I. Values of Effective Diffusivity, Mass Transfer Coefficient and Void Fraction

Diffusivity cm ² /sec	Mass Transfer Coefficient, sec ⁻¹	Source
(Naphthalene-Benzene)		
4.1	0.93 x 10 ⁻³	Meyer and Shen ¹²
3.9	0.91	Meyer and Shen
7.1	0.91	Meyer and Shen
5.2	0.58	Meyer and Shen
4.2	1.20	Meyer and Shen
(p-xylene--m-xylene)		
2.9	0.13 x 10 ⁻³	Meyer and Shen ¹²
3.1	0.15	Meyer and Shen
(Cyclohexane-Benzene)		
3.5		Albertins ¹
(m-Chloronitrobenzene-- m-Bromonitrobenzene)		
4.6	17.6 x 10 ⁻³	Gates ⁶
4.2	2.84	Gates
1.7	3.00	Gates
(Indole-Indene)		
14.8		Figure 17
10.0		Figure 18
6.5		Figure 19
4.0	1.1 x 10 ⁻³	Figure 22
<hr/>		
Void Fraction	Source	
0.46-0.53	Meyer and Shen ¹²	
0.479	McKay and Goard ¹⁰	

By applying the values of the approximate parameters, it can be established that

$$R_1 \gg R_2/R_1 \quad (23)$$

and that

$$R_1 h \gg 1.0 \quad , \quad (24)$$

therefore equation (19) can be approximated as:

$$y = -\frac{b_2}{m_2-1} + C_1 \exp(R_1 Z) + C_2 \exp(-R_2/R_1) Z \quad . \quad (25)$$

The constants C_1 and C_2 in equation (25) can be evaluated by using appropriate boundary conditions. The first boundary condition is the solution must be applicable at all conditions of operation. Specifically, the value of y must be between zero and one for all values of L . The second boundary condition is the composition of the liquid at $Z = 0$, i.e. $y = y_0$ (y_0 can be measured experimentally).

Examination of equation (17a) indicates that R_1 becomes very large as L increases or approaches zero. Because R_1 appears in the argument of the exponential, the term $C_1 \exp(R_1 h)$ would become exceedingly large under either of these conditions unless C_1 were small. In fact C_1 must be zero if y is to remain finite as L approaches zero. Application of the boundary conditions to equation (25) requires that:

$$C_1 = 0 \quad (26)$$

and

$$C_2 = y_0 + \frac{b_2}{m_2-1} \quad . \quad (27)$$

Coupling equations (25), (26) and (27), the following relation is obtained

$$y = -\frac{b_2}{m_2-1} + \left(y_0 + \frac{b_2}{m_2-1}\right) \exp\left(-\frac{R_2}{R_1} Z\right) \quad (28)$$

Equation (28) also predicts an exponential variation in composition with position in the crystallization column, but does not necessarily predict that y should approach a constant value at the upper end of a sufficiently long column.

Further simplification of equation (28) is possible for $(R_2/R_1)h \ll 1$. Under these conditions, with the further restriction that the equilibrium relation is a linear, equation (28) reduces to:

$$y = y_0 - (m_2 y_0 + b_2 - y_0) \frac{Z}{H} \quad (29)$$

$$H = \frac{\epsilon D \rho}{L} + \frac{m_2 L}{K a \rho} \quad (30)$$

This simplified expression, equation (29), predicts, subject to the assumptions incorporated in the development, that the composition of the liquid in a column crystallizer will vary linearly with position.

If the expression for H is multiplied by L , then the following linear relation between L^2 and HL results:

$$HL = \epsilon D \rho + m_2 L^2 / K a \rho \quad (31)$$

Thus the intercept and slope of a plot of HL vs. L^2 can be used to evaluate D and Ka .

4.0 EXPERIMENTAL STUDY

4.1 Equipment Description

The equipment used in this study is the same as that described by Meyer and Shen^{11,12}. Its main components are the column, a cooler-crystallizer, a stirrer, and a pulsing device (Figure 7).

The column was assembled from 15.24 cm sections of 5.08 cm ID Pyrex glass pipe separated by stainless steel sample and thermometer plates. Fixed to the lower end of the column was a stainless steel chamber which included a mercury seal. This seal prevented mixing of the column contents with the fluid in the hydraulic line connecting the column and the pulsing device. At the top of the column was a reservoir, in which the frozen discharge from the cooler-crystallizer was primarily separated. Excess liquid in the reservoir can be drawn off through a siphon at the top of the reservoir. The melting section was at the bottom; the necessary heat was supplied by heating tapes wrapped around the lower part of the column. Between the reservoir and the melting section, the purification section separated the two components of the binary mixture fed to the column.

Below the reservoir was a one way solids check valve which permitted concentrated slurry to be drawn into the purification section by a negative pressure pulse from the pulsing device. The combined action of the one way valve and pulsing device are shown schematically in Figure 8. During the positive pulse (pressure increasing in the column) melt (bottom product) is expelled from the bottom of the column while mother liquor and free liquid are forced out at the top of the column. Perforated members (20 by 150 mesh stainless steel screens) at both top and bottom held the crystals in the column while letting fluids escape.

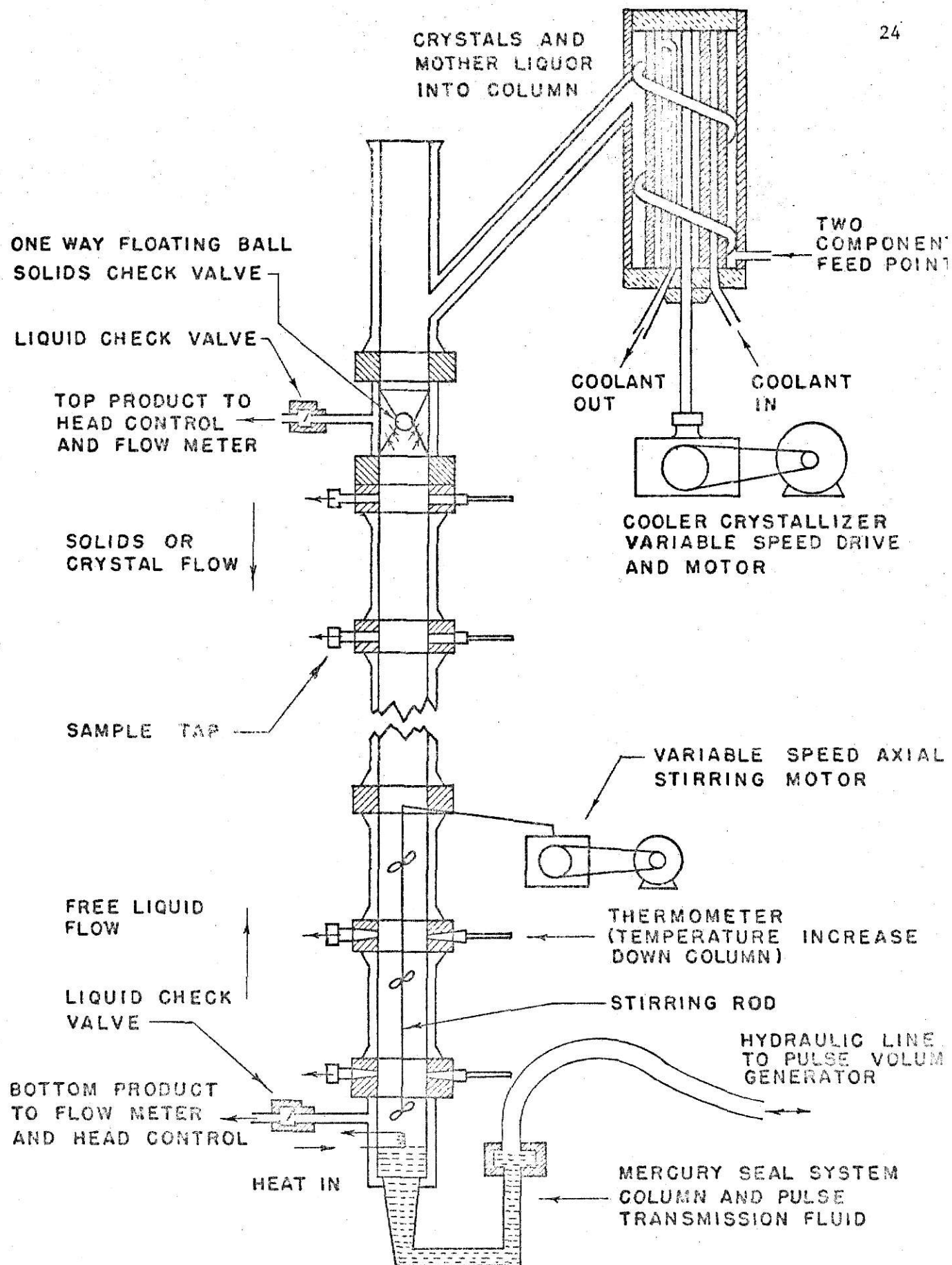


FIGURE 7: COUNTERCURRENT CONTINUOUS CRYSTALLIZATION SEPARATION AND PURIFICATION SYSTEM

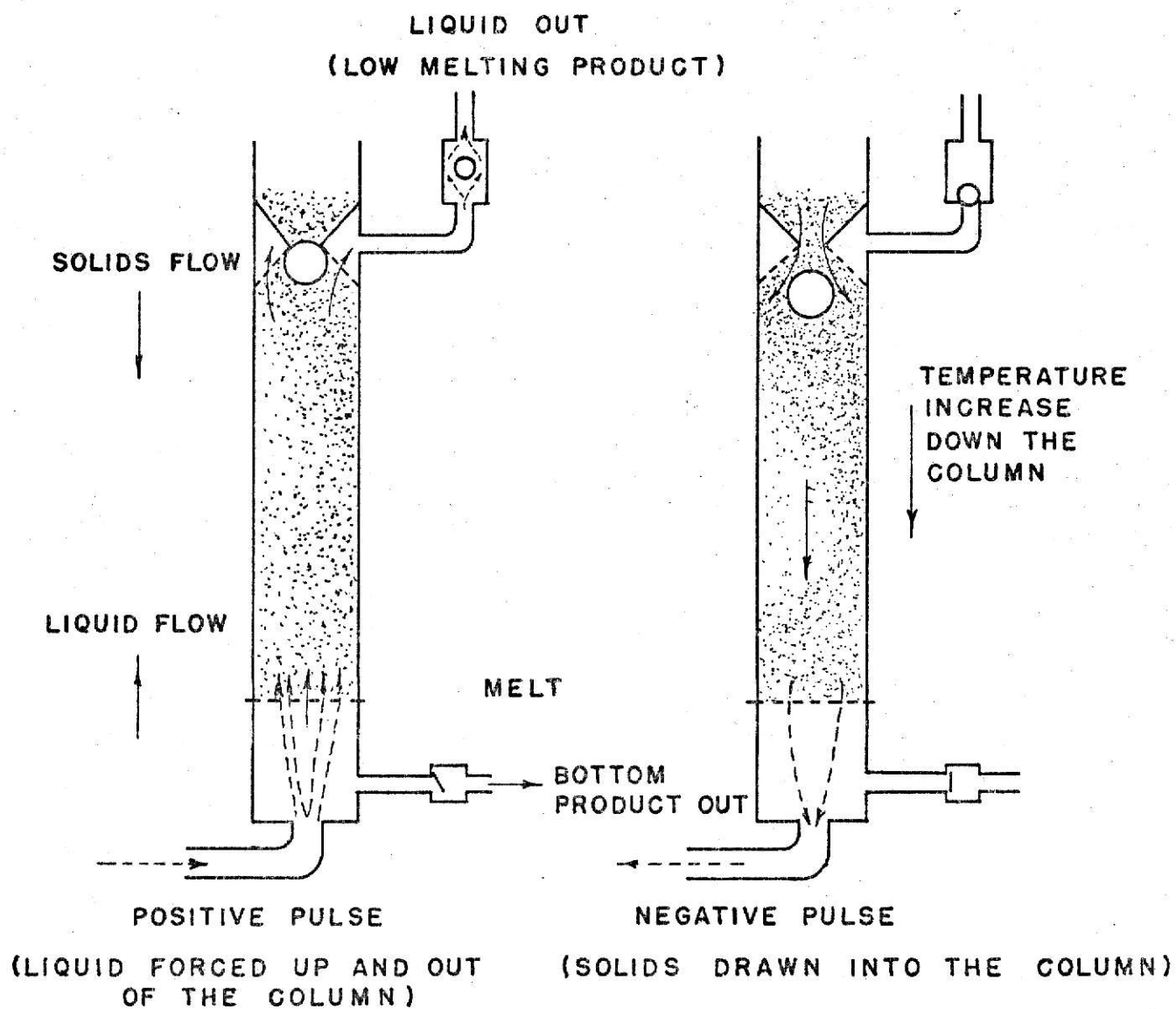


FIGURE 8: SOLIDS AND LIQUID PUMPING ACTION OF PULSE-CHECK VALVE COMBINATION

The cooler-crystallizer made of stainless steel, uses a helical conveyor to scrape both walls of the annular chamber it occupies to keep the walls free of crystals and to carry the newly formed crystals to the upper outlet of the unit. Alcohol circulated through the cooler-crystallizer as a coolant to remove latent heat of fusion from the feed stream. Coolant temperature is adjusted indirectly by the sublimation of dry ice in an alcohol bath, and the coolant rate is adjusted by a variable speed pump. A thermometer is installed upstream of the circulating pump to measure the coolant temperature. To facilitate the formation of a packed crystal bed in the column, two auxiliary cooling coils are wrapped around the bottom and 40 cm above the bottom, respectively. These are used only during column start up.

Operation of the column under approximately adiabatic conditions is achieved by insulating the glass column with no less than a 4 cm thickness of fiberglass.

The stirrer is driven by an outside variable speed motor. The stirrer operating at the axis of the column extends about 40 cm down to the bottom of the column.

4.2 Data Measurement Procedure

Liquid of the binary mixture being studied is charged to the column, and both stirrer and pulsing device are turned on. Coolant at a known temperature below the freezing point of the mixture is circulated through the two auxiliary cooling coils to form crystals in the lower part of the column. Crystals formed are agitated by the action of the stirrer and the pulsing device. About 30 minutes after initiation of operations the column will contain a slurry of crystals and liquid. The coolant is then switched to the cooler-crystallizer, and the binary feed solution is charged to the

cooler-crystallizer at a reduced feed rate. Soon after crystals are formed in the cooler-crystallizer and are discharged to the crystallization column, the feed rate is adjusted step by step until the desired feed rate is reached.

The rates of both bottom product withdrawal and reflux liquid circulation are adjusted as desired; the sum is equal to the feed rate. About two hours after the normal feed rate, and at least two hours subsequent to any significant adjustment in operating conditions, samples of the liquid in the column are removed through the sampling taps using a hypodermic needle and syringe. The weight of each sample is measured by difference on a Mettler type H5 electronic scale (NE 696).

4.3 Choice of System

The system chosen for this study was the solid-solution system indole-indene (Figure 9). The selection of this system was made because of the temperature limitation of the available equipment. Also phase equilibrium data were available for this system.

The indole-indene system has a very small separation factor. A feed containing 40 weight percent indole was fed to the cooler crystallizer; this composition was chosen based on the near room temperature saturation point (19.5°C). The known physical properties of indole-indene system are shown in Appendix A.

4.4 Quantitative Analysis of Column Samples

The samples removed from the crystallization column were analyzed quantitatively by a Packard Model 3375 Tri-Carb Scintillation Spectrometer.

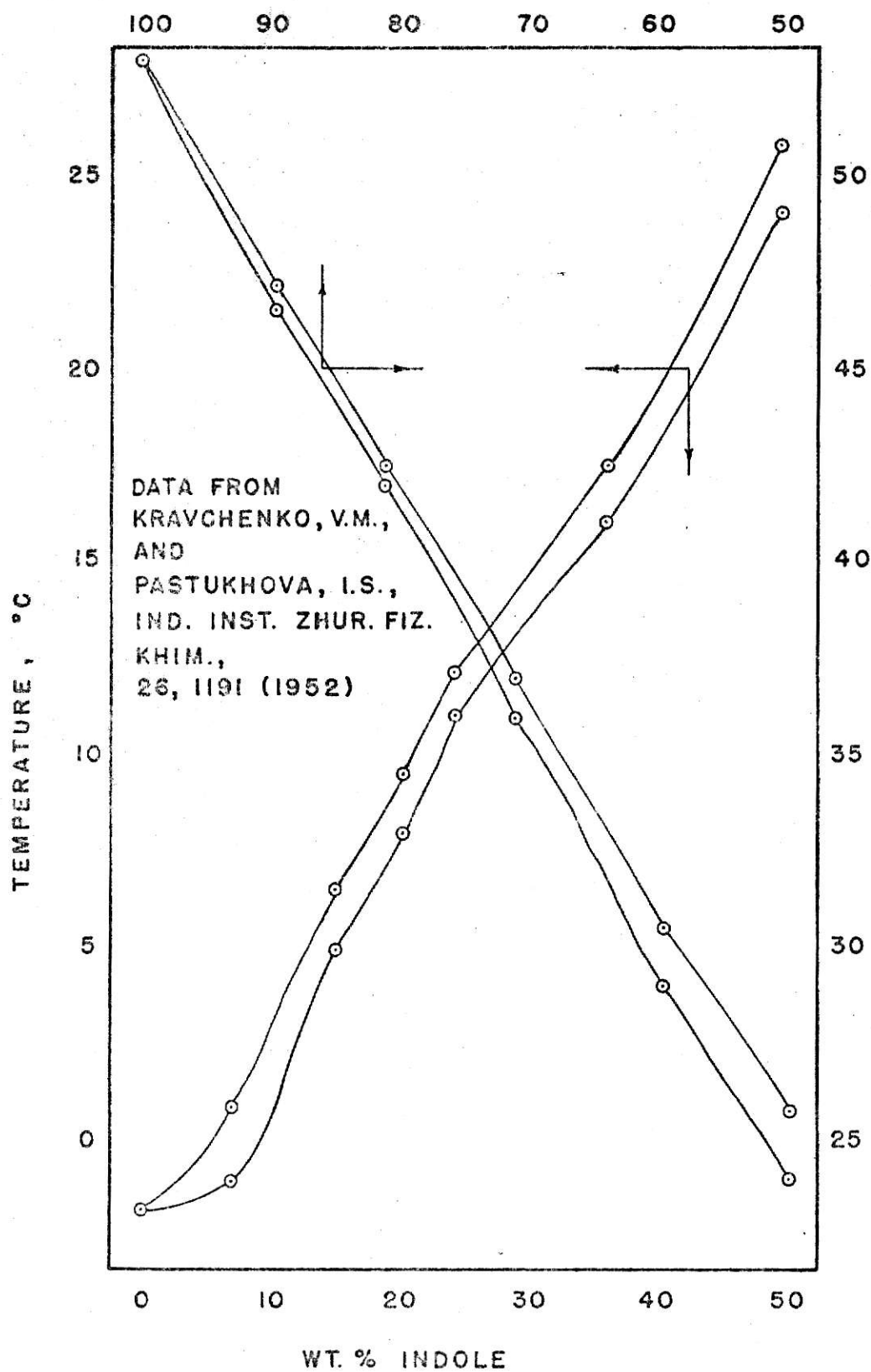


FIGURE 9: PHASE DIAGRAM OF INDOLE - INDENE

High melting component indole was tagged with radioactive Carbon-14 (a beta emitter with maximum disintegration energy of 156 Kev and half life of 5730 years) for counting purpose; the amount of tagged material used was 0.1 mCi (millicurie) of indole-2-C-14 in hexane added to the feed tank. To carry out the quantitative analysis, 0.1 gram samples were taken from the purification column and mixed with 15 ml of a commercially prepared organic scintillation counting solution in a special low background glass counting vial.

The overall counting efficiency of the liquid scintillation spectrometer is defined as the ratio of net counting rate CPM (counts per minute) to the sample true nuclide DPM (disintegrations per minute). An automatic external standardization system (AES ratio) is contained within the scintillation spectrometer to determine for any sample counted the counting efficiency. The net counting rate can be converted to DPM (normalized) as follows

$$\text{DPM} = \frac{\text{Observed mean CPM}}{\text{AEC indicated counting efficiency}}$$

A standardized calibration curve of the chemical system used in this study is shown in Figure 10.

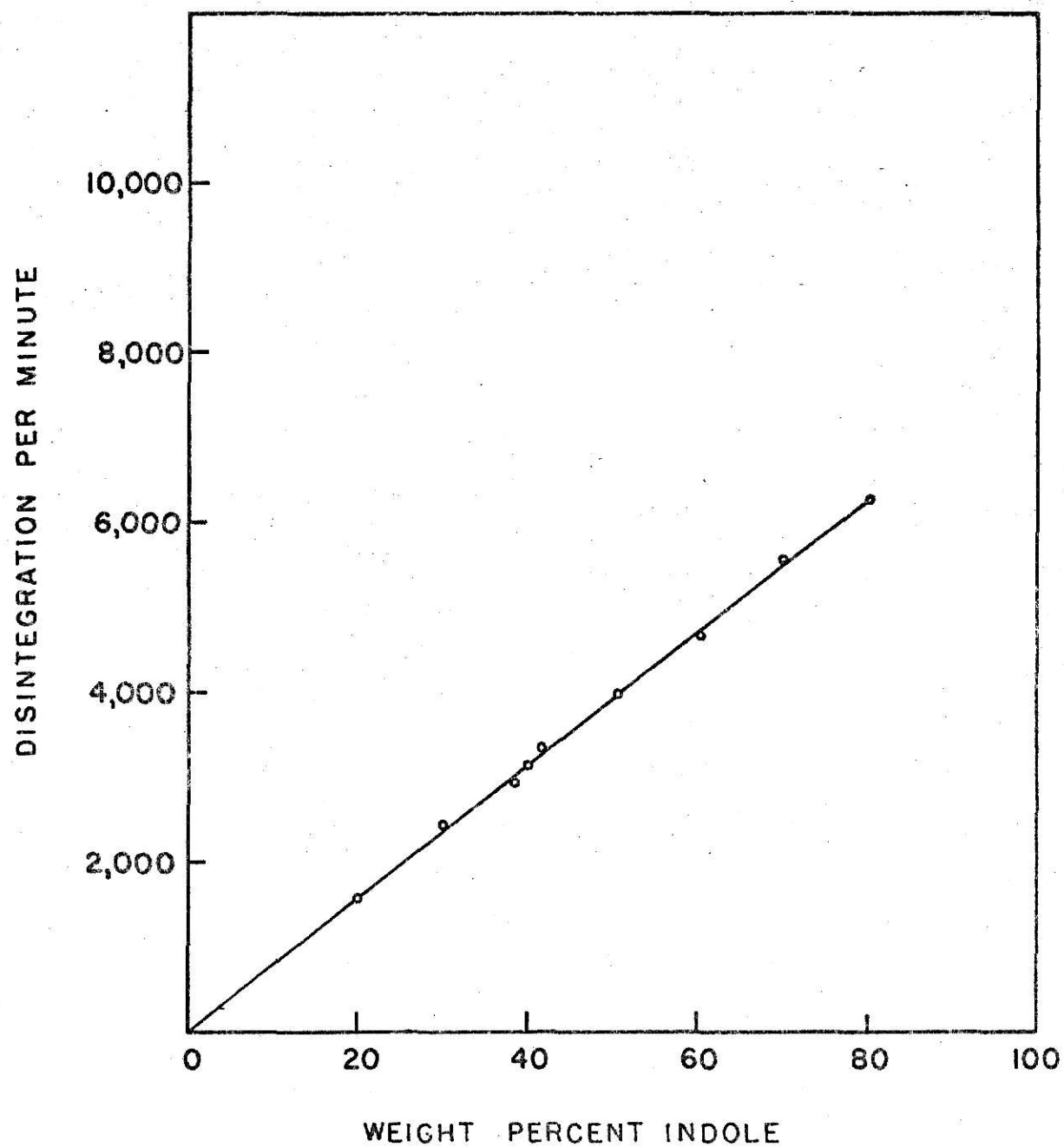


FIGURE 10 CALIBRATION OF STANDARD SAMPLE RADIOACTIVITY

5.0 EXPERIMENTAL RESULTS AND DISCUSSIONS

5.1 Experimental Results

The experimental results obtained in this study are summarized in Figures 11 through 16. These figures are plots of liquid composition vs. column position. The positions indicated are the location of sampling taps in the crystallization column: 0, 20, 60, and 80 cm above the bottom of the column. Figures 11 to 16 also show data at 90 cm above the bottom of the column; these data are based on analyses of the top product. Three samples were taken during sampling at each tap. The results shown are the arithmetical mean of the three measurements. The standard error of the arithmetical mean of the experimental was calculated as $\pm \sqrt{\frac{\sum R_i^2}{n(n-1)}}$, where R_i is the deviation of the i th measurement from the calculated arithmetical mean and n is the total number of samples taken at a particular sample tap during a particular measurement.

The operation variables pertaining to each data set are listed on the figures. The free liquid reflux rate was changed only slightly for the different runs described in the various graphs.

Within the limitation of the cooling capacity of the cooler-crystallizer unit, the separation achieved in the crystallization column increased with an increase in the free liquid reflux rate. At low free liquid reflux rates, the free liquid concentration profiles were rather flat.

5.2 Test of Experimental Column Performance with the Mass Transfer Limiting With Latent Heat Effect Model

The mass transfer limiting with latent heat effect model developed by Meyer and Shen^{11,12} is the result of the coupling of mass and energy continuity equations (3) and (4), but neglecting the interfacial heat transfer.

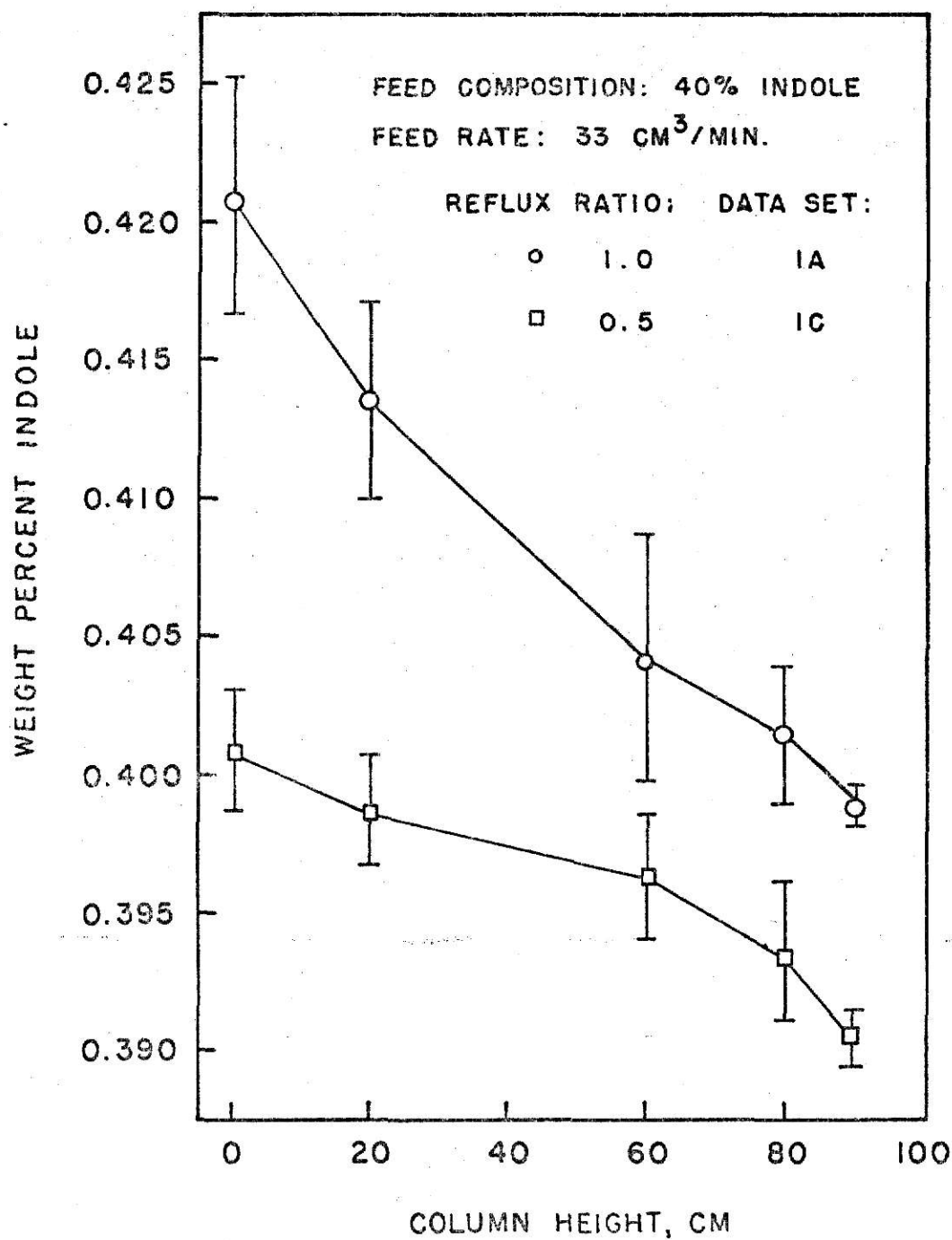


FIGURE II FREE LIQUID CONCENTRATION PROFILE OF DATA SET
IA AND IC

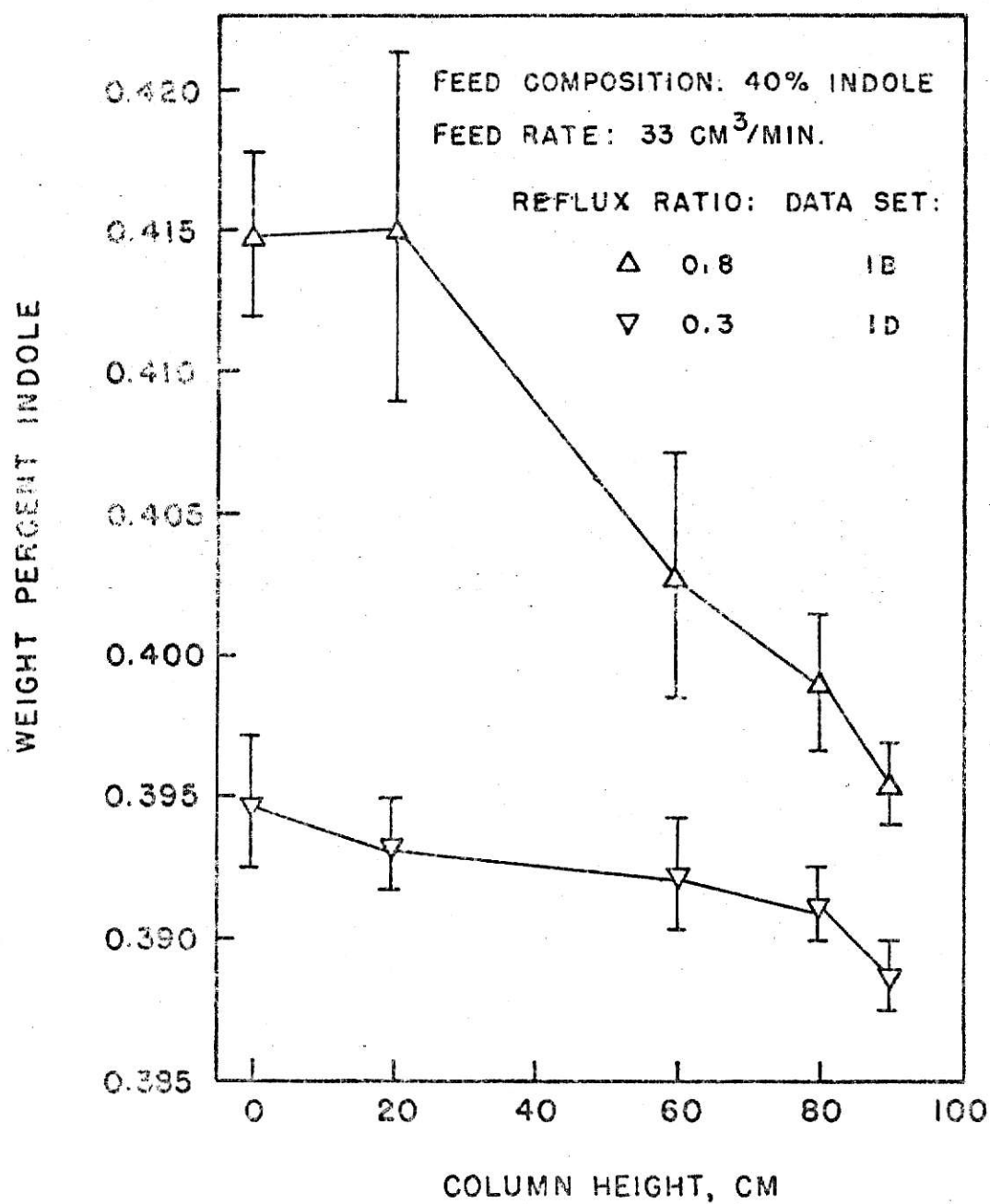


FIGURE 12 FREE LIQUID CONCENTRATION PROFILE OF DATA SET IB AND ID

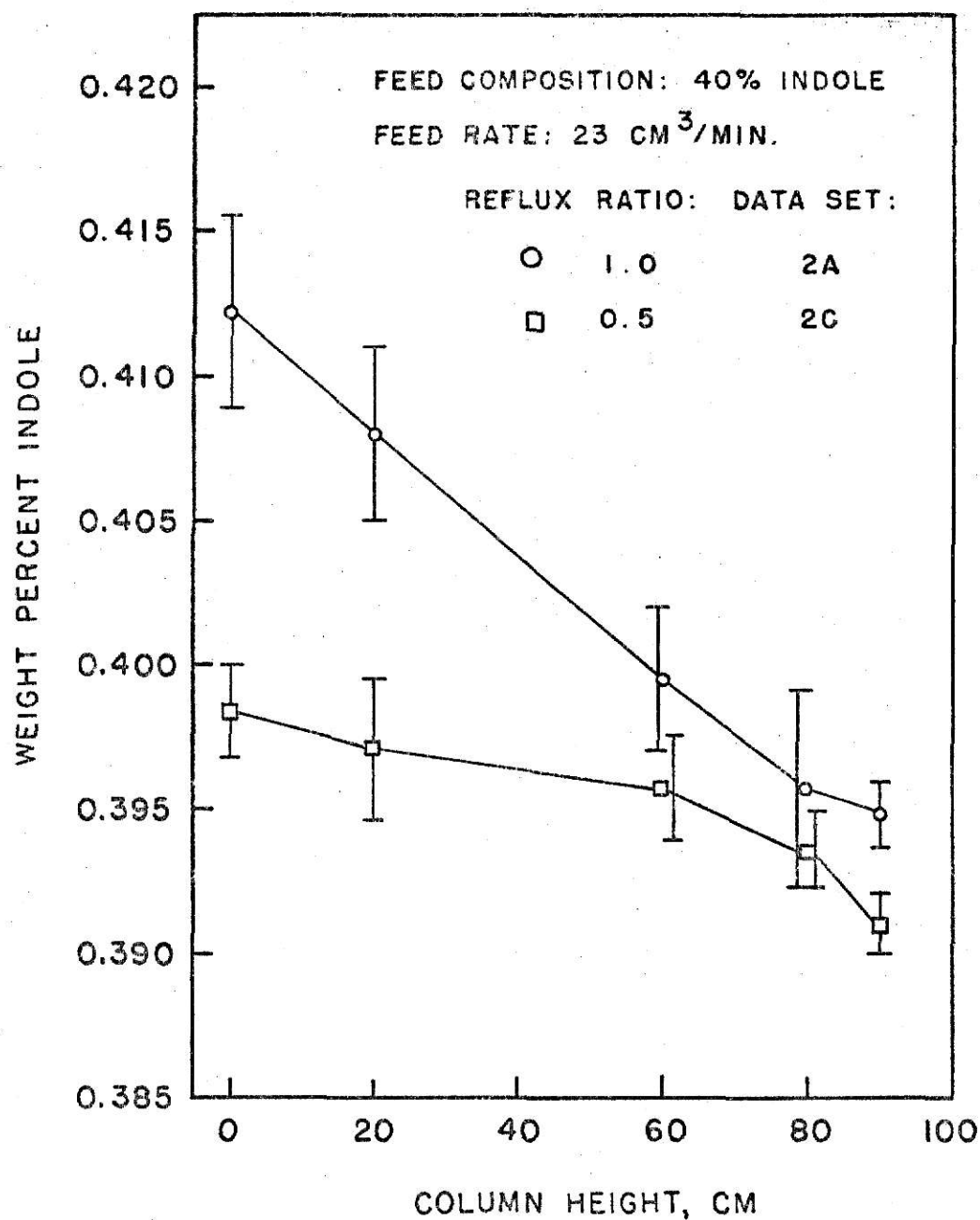


FIGURE 13 FREE LIQUID CONCENTRATION PROFILE OF DATA SET 2A AND 2C

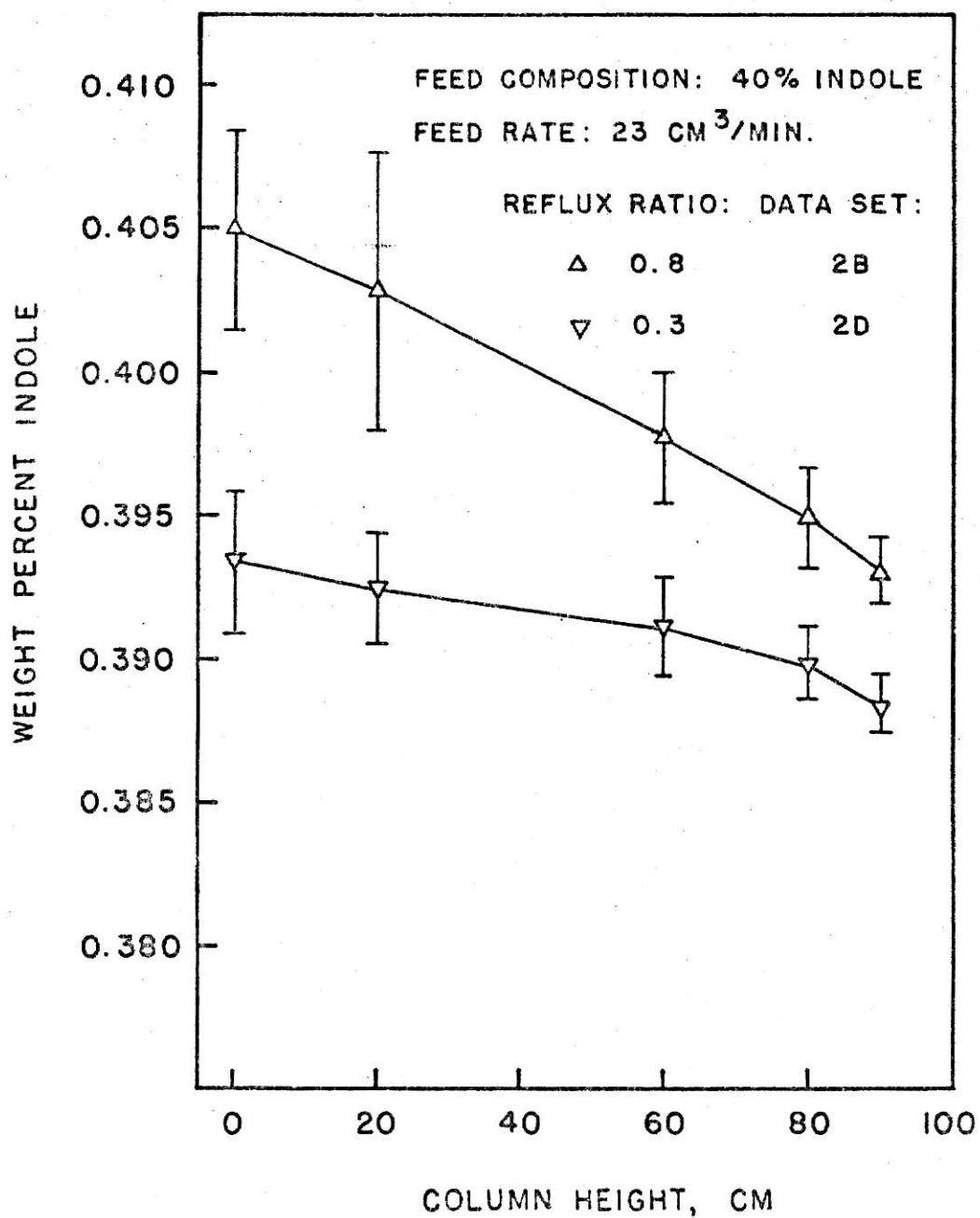


FIGURE 14 FREE LIQUID CONCENTRATION PROFILE OF DATA SET 2B AND 2D

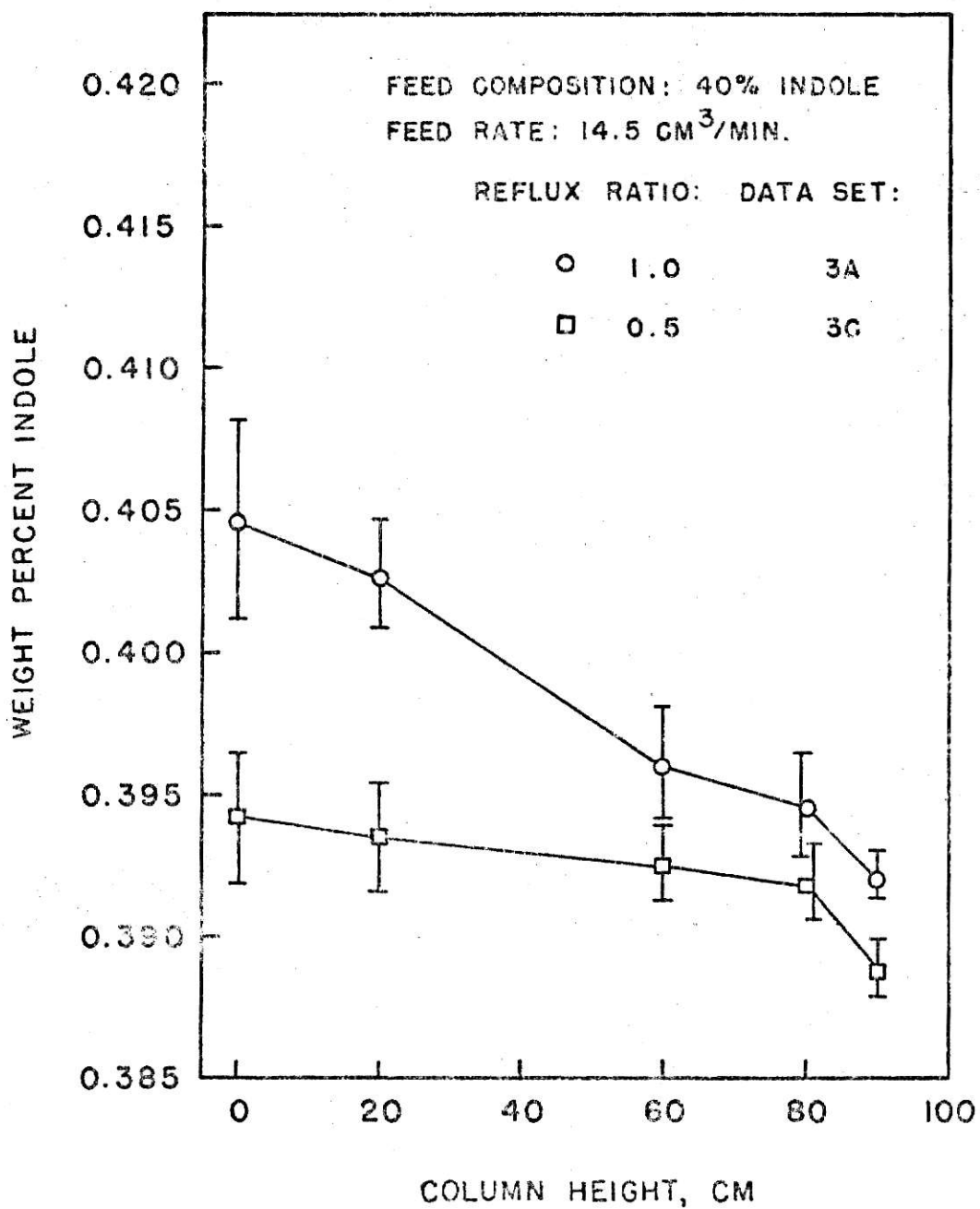


FIGURE 15 FREE LIQUID CONCENTRATION PROFILE OF DATA SET 3A AND 3C

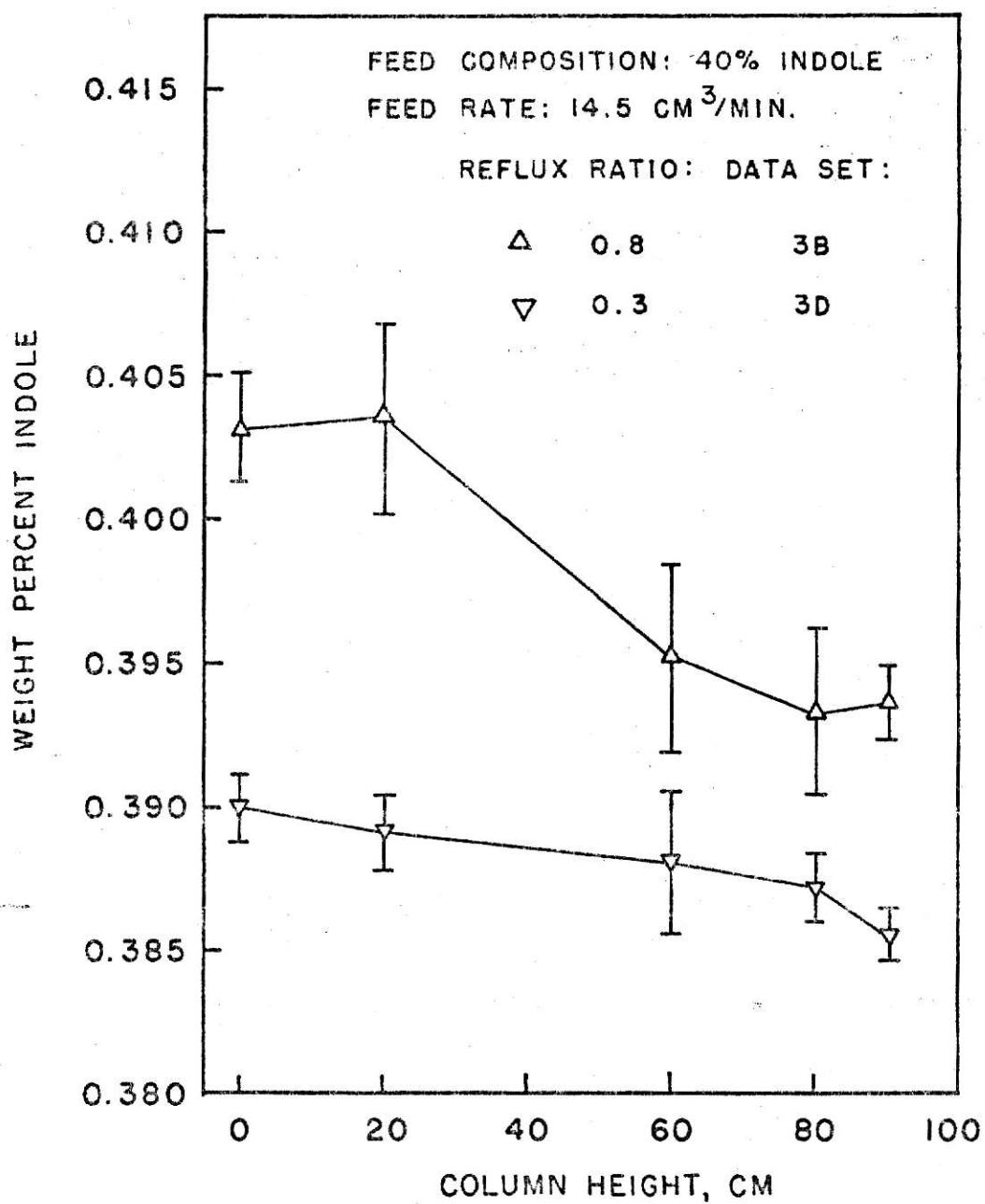


FIGURE 16 FREE LIQUID CONCENTRATION PROFILE OF DATA SET
3B AND 3D

The mass transfer limiting with latent heat effect model (see equations (11) and (12)) predicts an exponential variation of free liquid composition with position. A plot of the experimental data in the form of $\ln \left(\frac{y - y_f}{y_o - y_f} \right)$ vs. z should be a straight line with slope $(-A)$. The data of Figures 17 through 19 were fitted by a least squares method.

If the liquid density ρ , effective diffusivity D , and void fraction ϵ of equation (12) are not dependent on free liquid reflux rate for a column operating at total reflux (this is the assumption also made by Gates⁶), and if the specific heat C_p , the latent heat of fusion λ , and the slope of the temperature-concentration relation m_1 , for the indole-indene mixture are constant over a small range of composition, then the free liquid reflux rate will be the only factor affecting the value of A . Thus the experimentally determined A divided by V will be a constant, i.e.,

$$A/V = \frac{1}{\epsilon D \rho} \left(\frac{C_p}{\lambda m_1} - 1 \right) = \text{constant} \quad . \quad (32)$$

Figure 20 shows the results obtained when A , determined from Figures 17 through 19 is divided by V . A/V rather than being independent of free liquid flow rate appears to be an inverse linear functional of V . This result is in conflict with the mass transfer limiting with latent heat effect model, unless the assumption that the void fraction ϵ is independent of free liquid reflux rate is not true.

In developing the mass transfer limiting with latent heat effect model, the unknown mass transfer coefficient was eliminated from the mathematical formulation of the model by coupling the mass and energy continuity equations. Thus this model contains only the unknown axial effective diffusivity.

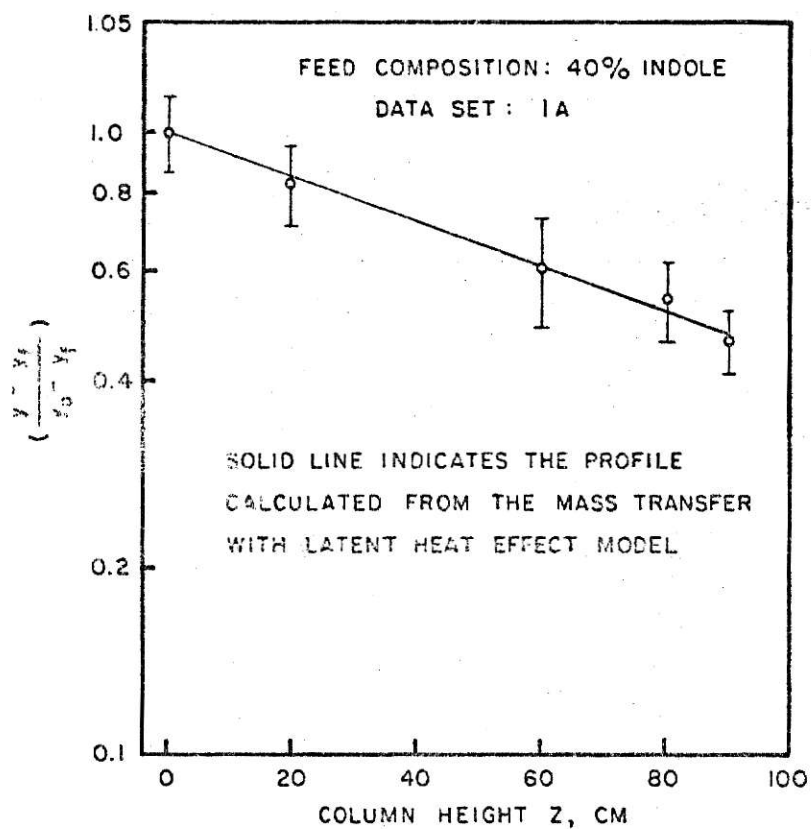


FIGURE 17 $\ln \left(\frac{y - y_f}{y_0 - y_f} \right)$ vs. Z MODIFIED FREE LIQUID
CONCENTRATION PROFILE OF DATA SET 1A

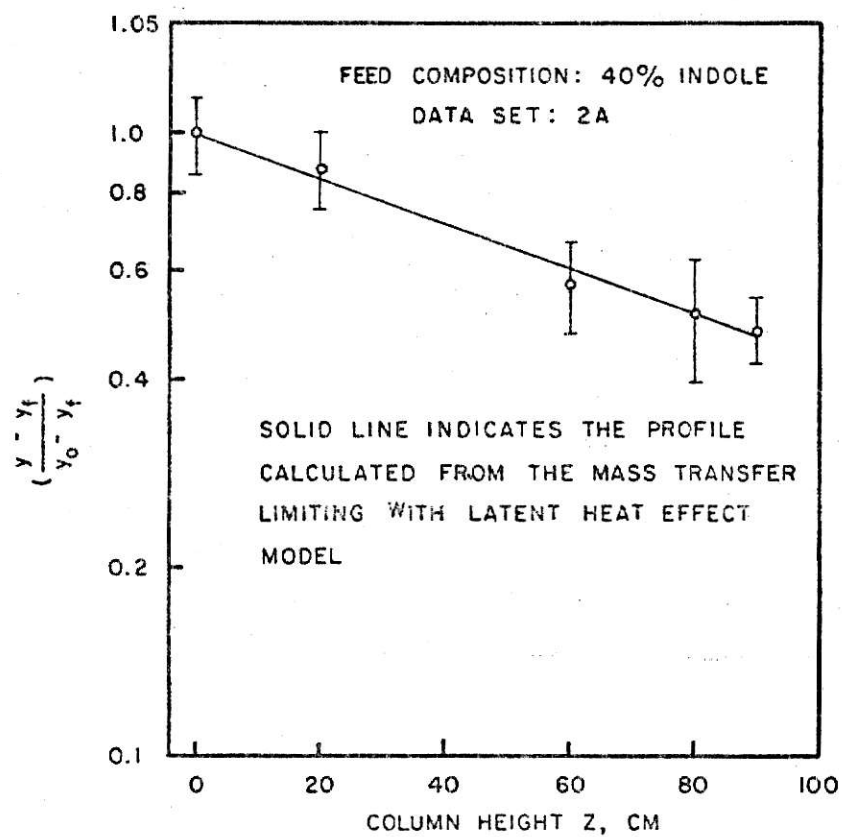


FIGURE 18 $\ln \left(\frac{y - y_f}{y_0 - y_f} \right)$ vs. Z MODIFIED FREE LIQUID
CONCENTRATION PROFILE OF DATA
SET 2A

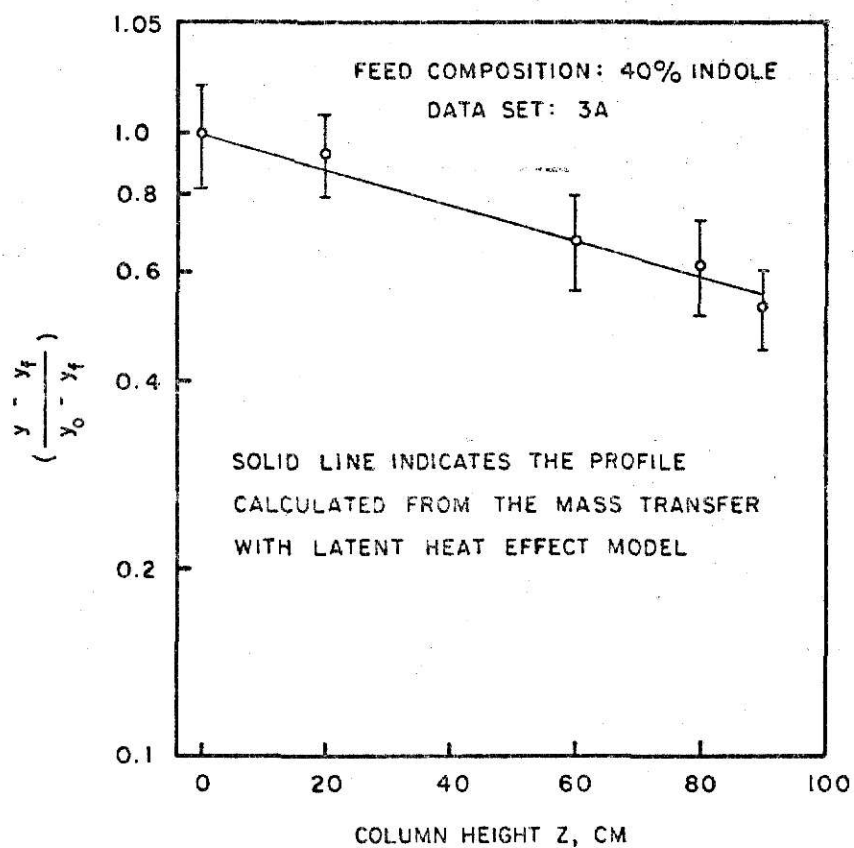


FIGURE 19 $\ln \left(\frac{y - y_f}{y_0 - y_f} \right)$ vs. Z MODIFIED FREE LIQUID
CONCENTRATION PROFILE OF DATA SET 3A

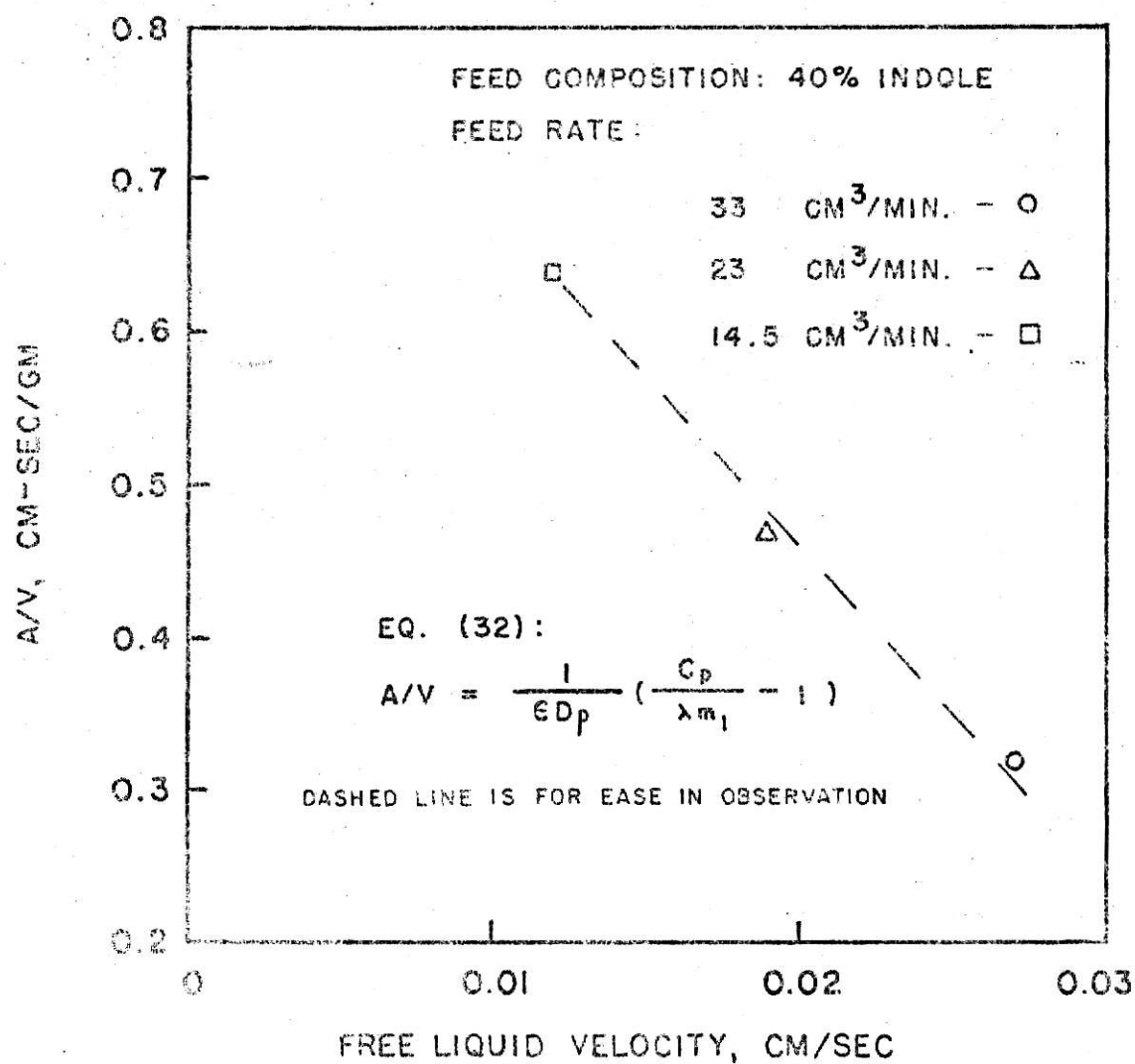


FIGURE 20 EXAMINATION OF PARAMETER A OF THE MASS TRANSFER LIMITING WITH LATENT HEAT EFFECT MODEL

In the mass transfer limiting with latent heat effect model, the effective axial diffusivity may be determined from the experimental concentration profile by plotting $-\ln\left(\frac{y - y_f}{y_o - y_f}\right)$ against the column height as shown in Figures 17 through 19. From the measured slope A, the effective axial diffusivity can be evaluated by equation (13). However, to separate and evaluate the axial effective diffusivity, the specific heat and the latent heat of fusion of the binary mixture being studied must be known. Unfortunately, this information for indole was not available. There are methods available to estimate the specific heat and the latent heat of fusion. Among them the additivity rules by Benson²⁷ and the estimation method suggested by Bauman³⁰ were used for the estimation of the specific heat and the latent heat of fusion of indole, respectively (see Appendices 3 and 4).

The measured effective diffusivities are shown in Table 1. The resulting diffusivities, 6.5 to 14.8 cm²/sec, are in fair agreement with the results obtained in pulsed extraction columns^{8,16} and also by Albertins¹, Gates⁶, and Meyer and Shen^{11,12}, which are ranged from low 0.5 to high 30 cm²/sec.

5.3 Test of Experimental Column Performance with the Mass Transfer Limiting Model

The mass transfer limiting model by Gates⁶ (see equations (29) and (30)) predicts a linear variation of free liquid composition with position for a column operating at total reflux. The line drawn on Figure 21 is the least squares line through the data points.

The mass transfer limiting model contains the term $(m_2 y_o + b_2 - y_o)$. As expressed in equation (16), $(m_2 y_o + b_2)$ may be regarded as the composition of an imaginary solid phase in equilibrium with y_o . The term $(m_2 y_o + b_2 - y_o)$

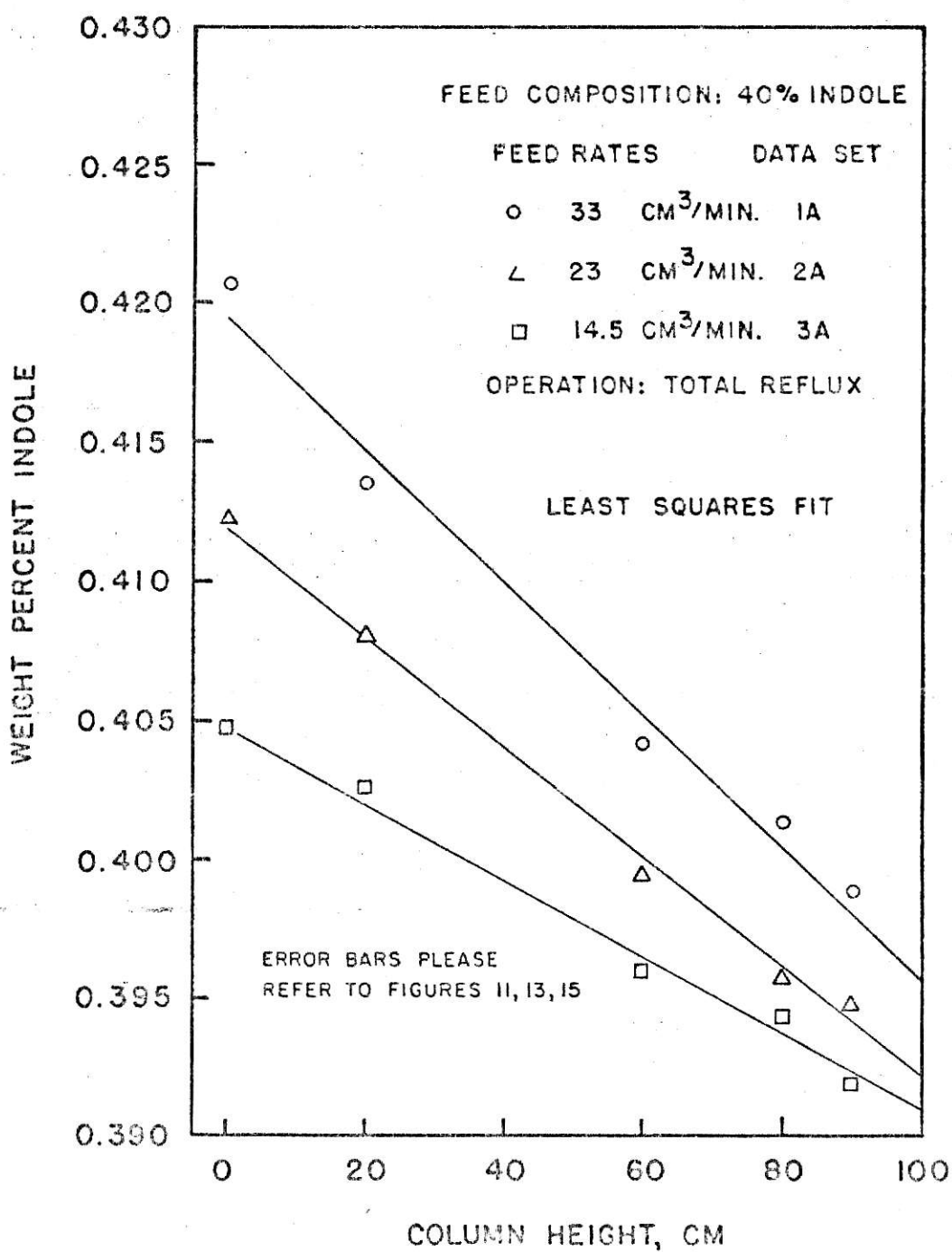


FIGURE 21 DETERMINATION OF THE PARAMETER H OF THE MASS TRANSFER LIMITING MODEL

relates the difference in composition between phases in equilibrium of an imaginary solid phase at the bottom of the column. Values of $(m_2 y_0 + b_2 - y_0)$ can be determined from the phase diagram together with the experimentally determined values of y_0 . The inclusion of the term $(m_2 y_0 + b_2 - y_0)$, the phase separation factor as defined by Gates⁶, predicts that the actual separation achieved in a crystallization column is proportional to the phase separation factor. The results as shown in Table II are comparable to those obtained by Gates⁶.

From equation (29), if the expression for H is multiplied by L , a linear relation between L^2 and HL results (see equation (31)). The intercept and slope of a plot of HL vs. L^2 can be used to evaluate D and Ka . Figure 22 illustrates such a plot. The data have been analyzed by a least squares method. Together with the estimated value for ϵ and calculated value for m_2 and ρ , the resultant value of D and Ka are shown in Table I. The calculated diffusivity, $4.0 \text{ cm}^2/\text{sec}$, is in fair agreement with published values for diffusivity determined in pulsed-column, liquid-liquid extraction columns^{8,16,17} and also by Albertins¹, Gates⁶, and Meyer and Shen^{11,12}.

The mass transfer limiting model predicts the influence of the crystal rate on the separation. At very low and very high rates, H is very large, and as a result, the separation is small. The separation passes through a maximum at some intermediate crystal rate. Due to the limitation of the cooling capacity of the cooler-crystallizer unit, the optimum crystal rate was not determined in this work. Within the range of the crystal rates which could be achieved, H decreased as the crystal flow rate increased (Figure 23). The observation is consistent with the fact that axial diffusion as represented by the group $(\epsilon D \rho / L)$ is more important than interphase mass transfer included

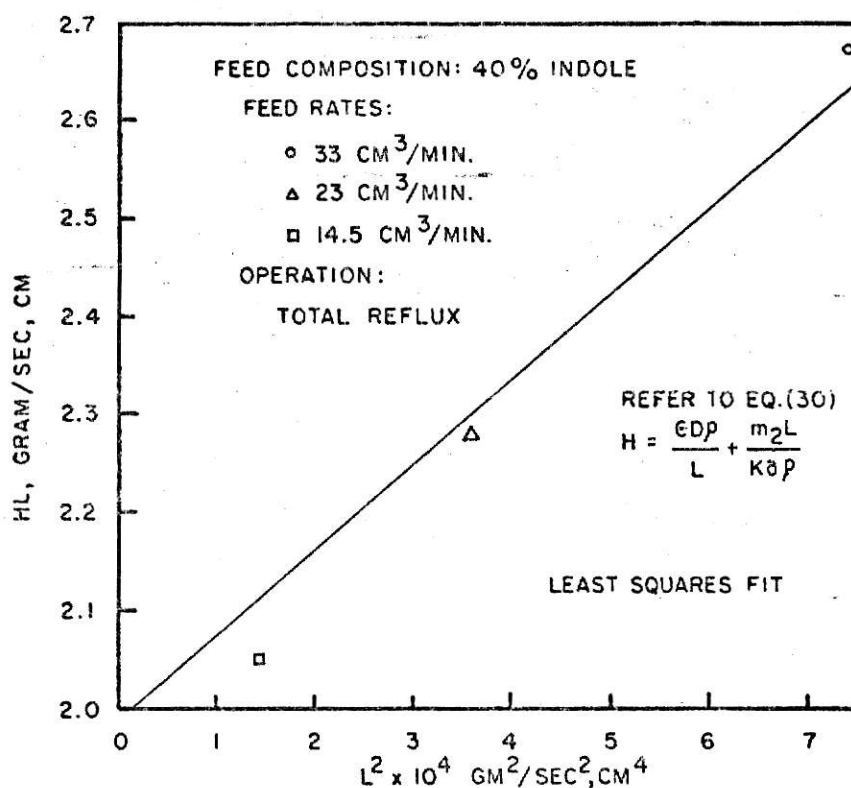


FIGURE 22 DETERMINATION OF DIFFUSIVITY AND MASS TRANSFER COEFFICIENT FOR INDOLE-INDENE — USING THE MASS TRANSFER LIMITING MODEL

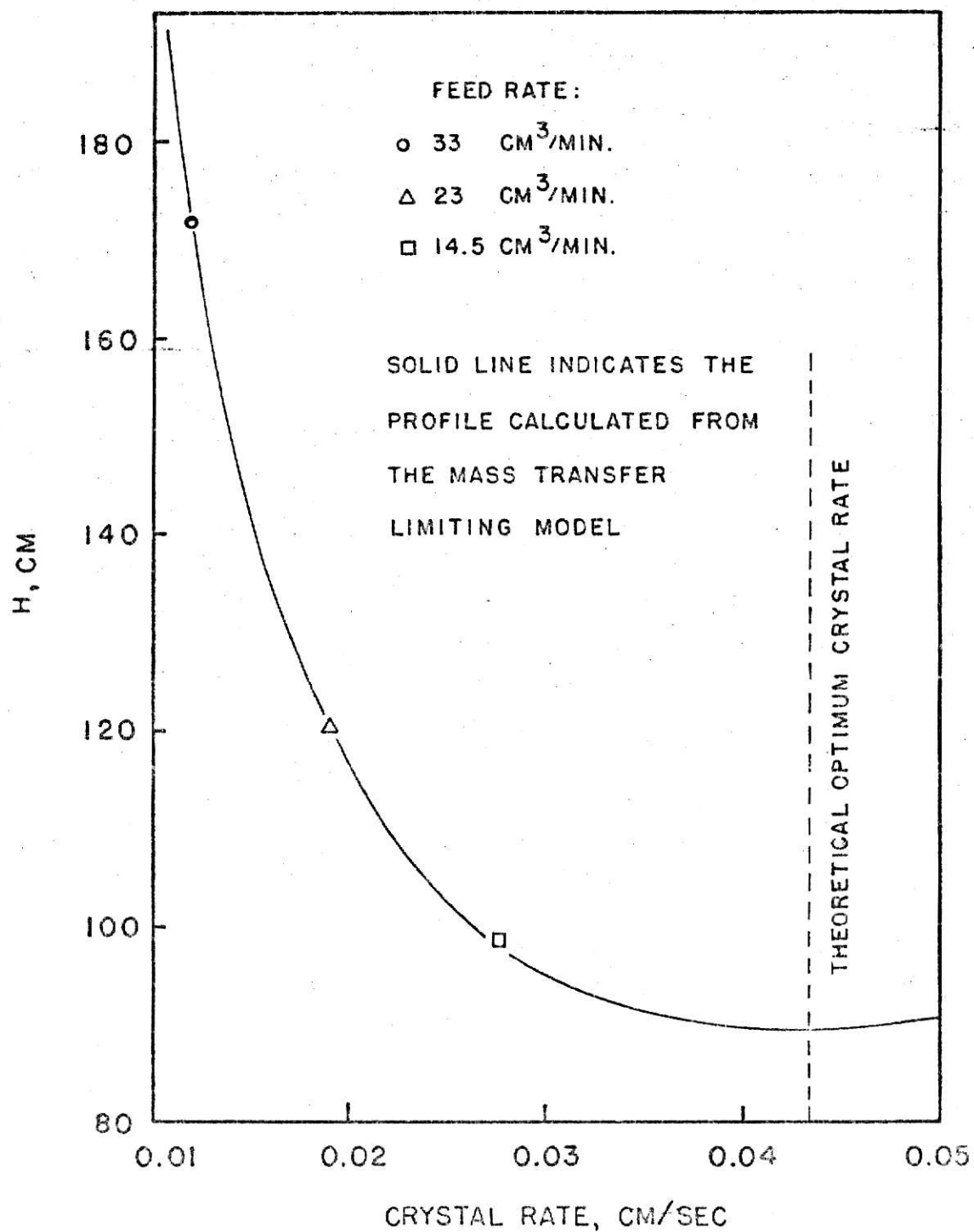


FIGURE 23 EFFECT OF CRYSTAL FLOW RATE ON SEPARATING ABILITY
COMPARISON OF EXPERIMENTAL AND CALCULATED VALUES
OF H FOR THE SYSTEM INDOLE-INDENE

in the group ($m_2/Ka\rho$). This conclusion is consistent with that obtained by Albertins¹ and Gates⁶.

Figure 23 is also a comparison of experimental and calculated values of H as a function of crystal flow rate for the system indole-indene. The effective diffusivity, D , and the mass transfer coefficient, Ka , determined from Figure 22 together with equation (28) are adequate to represent the behavior of the columns as illustrated in Figure 23.

5.4 Effect of Reflux Ratio on Free Liquid Concentration Profile.

To examine the effect of the liquid phase on the purification process, experiments were conducted in which the free liquid reflux ratio was varied. The reflux ratio is defined as:

$$R = \frac{\text{Weight of liquid forced up the column}}{\text{Weight of bottom product at zero reflux}}$$

The experimental results as illustrated in Figures 11 through 16 showed that the concentration profile of the free liquid is flatter the lower the reflux ratio. The separation achieved is also smaller for small reflux ratios.

The mass transfer limiting model assumes the crystallization column is operated at total reflux. The model cannot be applied to explain the behavior of the column operated at partial reflux.

The mass transfer limiting with latent heat effect model is independent of solid phase variables. This model predicts an exponential variation in the free liquid composition with position. The free liquid reflux rate as a variable is contained in the parameter A in the exponential term of equation 12. Thus the observed flatness of the free liquid concentration profile at a low reflux ratio operation is also qualitatively in agreement with the mass transfer limiting with latent heat effect model.

Table II. Influence of Difference in Phase Compositions on Separation

Phase Separation Factor	Separation	Crystal Rate g/sec, cm ²	Source
0.0235	0.022	0.027	Figure 15
0.0235	0.017	0.019	Figure 16
0.0235	0.013	0.012	Figure 17
~0.01	0.015	0.080	Gates run 13
0.037	0.089	0.076	Gates run 29
0.039	0.089	0.066	Gates run 30
0.039	0.070	0.050	Gates run 31
0.057	0.055	0.072	Gates run 14
0.057	0.080	0.072	Gates run 15
0.058	0.106	0.054	Gates run 16
0.059	0.072	0.036	Gates run 17
~0.01	0.005	0.024	Gates run 6
~0.01	0.005	0.018	Gates run 7

The free liquid concentration profiles as illustrated in Figures 11 through 16 indicate that a sharp change in concentration gradients was noted at the top of the column under partial reflux operations. The sharp discontinuity in the concentration and temperature profiles have been reported by Player¹⁴, Meyer and Shen¹² and others¹⁰ who have studied the end-fed type Philips purification column for the separation of m-xylene--p-xylene.

The sharp change in the concentration and temperature profiles is a phenomena only observed in end-fed columns. This phenomena was not reported in center-fed columns.

Mechanisms involved in the operation of the crystallization column are expected to be washing and refreezing¹⁹. Washing is the mechanism by which the impurities in the liquid adhering to the crystals are reduced for transfer into the free liquid. Refreezing is the mechanism by which impurities are removed from the crystals (as the result of repeated phase changes in the free liquid and in the solid phase).

Player implied that the sharp change in the concentration and temperature profiles is related to the refreezing of the reflux liquid. He suggested that there will be a restriction on the quantity of reflux which will produce such a discontinuity. Schildknecht type center-fed columns are not operated with a compact bed of crystals, and in a column operated under total reflux conditions, the reflux rate is clearly in excess of that maximum which could be refrozen to form a sharp discontinuity in temperature and composition. Player expected that these factors are among the reasons why a sharp change in the concentration and temperature profile is not observed in center fed columns.

The refreezing of liquid reflux at the top of end-fed columns operating at a reduced free liquid reflux rate leads to the assumption by Player that the free liquid reflux rate and the value of the void fraction would decrease

along the column. Free liquid reflux rate is closely related to the value of the void fraction and would be in direct proportion to the void fraction. Based on this observation, the mass transfer limiting with latent heat effect model could well explain the results shown in Figure 20. If the value of the void fraction decreases with a decrease in free liquid reflux rate, the value of A divided by V will increase with a decrease in the free liquid reflux rate. Figures 24 and 25 give qualitative illustration of the relation.

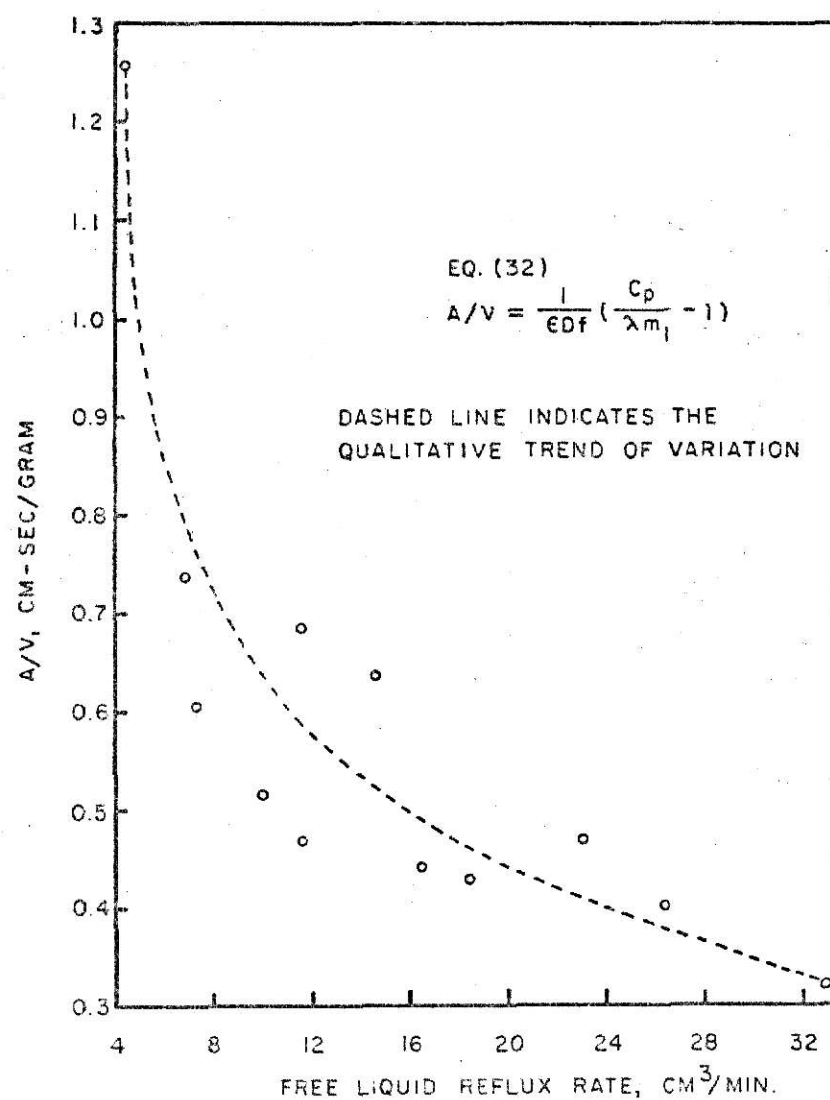


FIGURE 24 QUALITATIVE ILLUSTRATION OF THE RELATION BETWEEN A/V AND FREE LIQUID REFLUX RATE

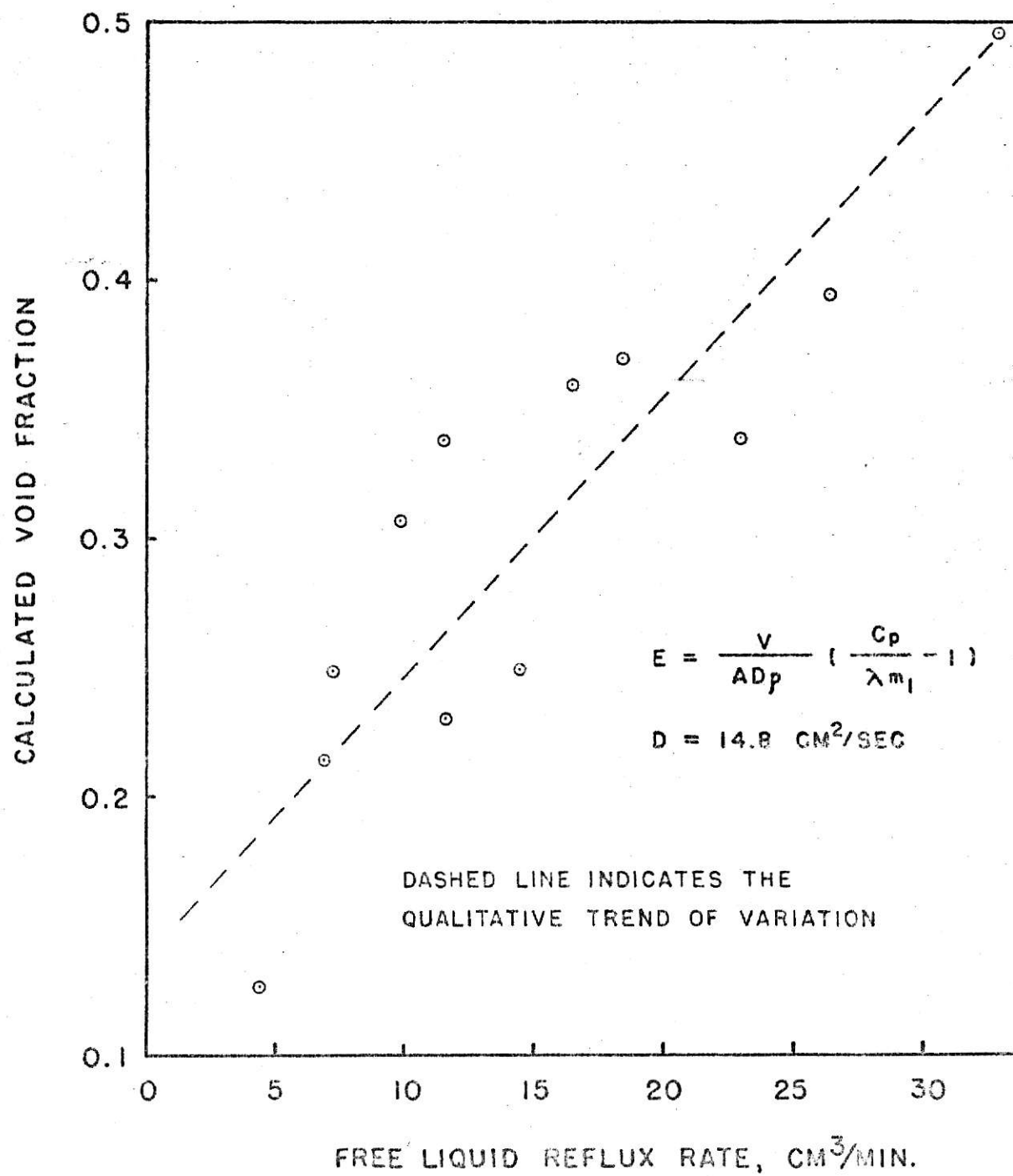


FIGURE 25 QUALITATIVE ILLUSTRATION OF THE RELATION BETWEEN VOID FRACTION AND FREE LIQUID REFLUX RATE

6.0 CONCLUSIONS

The experimental concentration profiles measured for the free liquid in a countercurrent column crystallizer operating at total reflux on the solid solution system indole-indene are in fair agreement with predictions made by both the mass transfer limiting with latent heat effect and the mass transfer limiting mathematical models. The measured effective diffusivities obtained by application of these two models are also in agreement with the results obtained in pulsed extraction columns^{8,16} and also by Albertins¹, Gates⁶, and Meyer and Shen^{11,12}.

The mechanisms involved in the operation of a crystallization separation column are expected to be washing and refreezing; washing is a hydrodynamic process. Refreezing is the result of phase changes in the free liquid and in the solid phase. Heat transfer effects are expected to be much more important for refreezing than for washing. In the case of a crystallization column operating at total reflux, Player¹⁴ suggested that if the reflux rate were in excess of that maximum which could be refrozen, washing will be the dominant mechanism leading to separation in the crystallization column.

The experimentally measured separation of the solid solution system indole-indene was low, thus the concentration of the binary mixture along the column was about the same. Under these conditions the values of the specific heat and the latent heat of fusion of the binary mixture would be expected to remain essentially constant along the column and thus no significant heat transfer effect would be present in the crystallization-separation process. Therefore at total reflux operation the mass transfer limiting with latent heat effect model and the mass transfer limiting model would be effectively the same (both models are derived from the same mass continuity

equation). Thus, both the mass transfer limiting with latent heat effect model and the mass transfer limiting model are suitable for correlating the experimental concentration profile obtained for the solid solution system indole-indene operated at total reflux.

The mass transfer limiting model by Gates⁶ fails to predict the sharp change in concentration profile at the top of the column under partial reflux operations. Player¹⁴ expected that the sharp change in concentration profile is related to the refreezing of the reflux liquid. The observation of the sharp change in concentration and temperature profiles indicated to Player¹⁴ that the assumed constancy of the free liquid reflux rate along the column was not actually present.

7.0 ACKNOWLEDGEMENTS

The author wishes to express his most sincere gratitude to Dr. W. Meyer for his stimulative guidance, helpful suggestions and encouragement throughout the course of this study. Gratitude is extended to the Department of Nuclear Engineering and the Kansas State University Engineering Experiment Station for financial support of this research.

8.0 REFERENCES

1. R. Albertins and J. E. Powers, "Experimental and Theoretical Investigation of Purification in a Column Crystallization of the Eutectic Forming Type," *AIChE Journ.* Vol. 15, No. 4, 554 (1969).
2. Anon., "Model 3375 Tri-Carb Liquid Scintillation Spectrometer Operation Manual," Packard Instrument Co., (1966).
3. J. S. Ball, R. V. Helm and C. R. Ferrin, "Zone Melting-New Purification Tool," *Petrol. Engg.* 30(13), C36, (1958).
4. M. Benedict and T. H. Pigford, "Nuclear Chemical Engineering," McGraw-Hill inc., New York (1957).
5. R. B. Bird, W. E. Stewart and E. N. Lightfoot, "Transport Phenomena," John Wiley and Sons, Inc., New York (1960).
6. W. C. Gates, Jr., "Determination of Mechanisms Causing and Limiting Separations in Column," Ph.D. Dissertation, University of Michigan (1970).
7. J. D. Henry, Jr. and J. E. Powers, "Experimental and Theoretical Investigation of Continuous Flow Column Crystallization," *AIChE Journ.* Vol. 16, No. 6, 1055 (1970).
8. S. C. Jones, "On the Behavior of a Pulsed Extraction Column" Ph.D. Dissertation, The University of Michigan (1963).
9. D. L. McKay, G. H. Dale, and J. A. Weedman, "A Bench-Scale Crystallization Purification Column," *Ind. Engg. Chem.*, Vol. 52, No. 3, 197 (1960).
10. D. L. McKay and H. W. Goard, "Continuous Fractional Crystallization," *Chem. Engg. Prog.*, Vol. 11, 99 (1965).
11. W. Meyer and P. K. Shen, "Separation and Purification by Continuous Countercurrent Crystallization," Paper presented at the Symposium on Selected Papers--Part I, Sixty-fourth National Meeting, New Orleans, Louisiana, March 16-20, (1969).
12. W. Meyer and P. K. Shen, "Crystallization from the Melt: Design Models for Separation of Eutectic Systems by Continuous Countercurrent Columnar Crystallization," Paper presented to AIChE National Meeting, Chicago, Illinois, Nov. (1970).
13. J. W. Mullin, "Crystallization," Butterworths, London, (1961).
14. M. R. Player, "Mathematical Analysis of Column Crystallization," *Ind. Eng. Chem. Proc. Des. Develop.*, Vol. 8, No. 2, 210 (1969).

15. S. H. Redgrove, "Indole," *The Perfumery and Essential Oil Record*, 161, May (1929).
16. L. D. Smott and A. L. Babb, "Mass Transfer Studies in a Pulsed Extraction Column," *Ind. Eng. Chem. Fund.*, Vol. 1, No. 2, 93 (1962).
17. G. Thorsen and S. O. Terjesen, "On the Mechanism of Mass Transfer in Liquid-Liquid Extraction," *Chem. Eng. Sci.*, Vol. 17, 137 (1962).
18. R. C. Weast, "Handbook of Chemistry and Physics," The Chemical Rubber Company, Cleveland, Ohio (1968-1969).
19. M. Zief and W. R. Wilcox, "Fractional Solidification," Vol. 1, Marcel Dekker, Inc., New York (1967).
20. A. Zielenkiewicz, "Enthalpy of Evaporation and Average Specific Heat of Nitromethane, Indene, Coumarone, and Mesitylene," *PRZEMYST CHEM.*, 44/12 664 (1965).
21. V. M. Kravchenko and I. S. Pastukhova (N.S. Khrushchev Donets) Inc. *Inst. Zhur. Fiz. Khim.*, 26, 1191 (1952).
22. P. M. Arnold, U. S. Patent 2,540,997 (February 6, 1951).
23. J. E. Powers, "Column Crystallization: Phenomenological Theory," Paper presented to the Symposium on Zone Melting and Column Crystallization, Karlsruhe, Germany, June 5-7, 1963.
24. J. A. Weedman and R. A. Findlay, *Petrol. Refin.*, 37, 195 (1958).
25. A. Aihara, "Studies on Hydrogen Bondings by Means of the Determination of Vapor Pressure," *J. Chem. Soc. Japan, Pure Chem. Sect.*, 76, 497 (1955).
26. V. V. Serpinski, S. A. Voitkevich and N. Yu. Lyuboshits, (All-Union Sci. Research Inst. Synthetic and Nat. Aromatic Principles, Moscow), "Determination of the Saturated Vapor Pressure of Several Fragrant Substances," *Zhur. Fiz. Khim.*, 28, 810 (1954).
27. R. Shaw, "Heat Capacity of Liquids: Estimation of Heat Capacity at Constant Pressure and 25°C Using Additivity Rules," *Journ. of Chem. and Eng. Data*, Vol. 14, No. 4, 461 (Oct. 1969).
28. J. H. Perry, "Chemical Engineering Handbook," 3rd Ed. (1960).
29. D. M. Scott, W. T. Berg, I. A. Hossenlopp, W. N. Hubbard, L. F. Messerly, S. S. Todd, D. R. Douslin, J. P. McCullough, and G. Waddington, "Pyrrole: Chemical Thermodynamic Properties," *J. Phys. Chem.* 71(7), 2263 (1967).
30. E. Bauman, "Prediction for Soviet Physical and Physico-chemical Properties of Chemical Compounds," *NAFTA BROJ* 11, 335 (Nov. 1956).

31. H. Kallmann, "Scintillation Counting With Solutions," Phys. Rev., 78, 621 (1950).
32. S. W. Benson, J. Chem. Phys. 15, 866 (1947).
33. S. W. Benson, F. R. Cruickshank, D. M. Golden, G. R. Hangen, E. H. O'Neal, A. S. Rodgers, R. Shaw, R. Walsh, Chem. Rev., 69, 279 (1969).

9.0 APPENDICES

Appendix A

Physical Properties of Indole-Indene System.

1. Density of Indole in Indene

Indole	20°C	0.9968 gram/cm ³
--------	------	-----------------------------

Indene	20°C	0.9915 gram/cm ³
--------	------	-----------------------------

For an indole-indene mixture, the density of the mixture is calculated by the following equation which assumes a linear relation between composition and density:

$$d_s = \frac{d_n d_o}{d_n C + (1-C)d_o} ,$$

d_s , d_n and d_o are the density of the system, pure indene and pure indole respectively and C is the weight fraction of indole in the system. For $C = 0.4$, $d_s = 0.9936$ gram/cm³.

Reference: R. C. Weast, "Handbook of Chemistry and Physics,"
48th Ed.

2. Heat Capacity

Indene	20.63 to 64.37°C	0.393 cal/g. °C
--------	------------------	-----------------

Reference: A Zielenkiewicz, PRZEMYST CHEM. 44/12, 664 (1965).

3. Heat of Fusion

Indene	19.9 cal/gram
--------	---------------

Reference: Klatt, Z. Physik. Chem. A171 454 (1934).

4. Heat of Vaporization

Indene	8.50 Kcal/g-mole
--------	------------------

Reference: A. Zielenkiewicz, PRZEMYST CHEM. 44/12, 664 (1965).

Indole 17.9 Kcal/g-mole

Reference: V. V. Serpinski, et al., Zhur. Fiz. Khim, 28, 810
(1954).

5. Heat of Sublimation

Indole 16.73 Kcal/g-mole

Reference: A. Aihara, J. Chem. Soc. Japan, Pure Chem. Sect., 76,
497 (1955).

6. Vapor Pressure

Indole $\log p \text{ (mm Hg)} = 10.334 - 3655.4 T^{-1} \text{ (}^\circ\text{K)}$

Reference: A. Aihara, J. Chem. Soc. Japan, Pure Chem. Sect.,
76, 497 (1955).

Appendix B




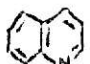
Phase Equilibrium Data of Indole-Indene System²¹

Mole Fraction Indole	Weight Fraction Indole	°C	°C
1.000	1.0000	52.9	53.0
0.895	0.8960	46.5	47.1
0.808	0.8096	42	42.5
0.707	0.7090	36	37.0
0.592	0.5940	29	30.5
0.494	0.4964	24	25.8
0.359	0.3610	16	17.5
0.248	0.2494	11	12.1
0.203	0.2041	8	9.5
0.151	0.1515	5	6.5
0.071	0.0718	-1	0.9
0.000	0.0000	-1.8	-1.7

Appendix C

Estimation of Heat Capacity of Liquids by the Additivity Rules

The additivity rules are due to Benson³². He observed that the contribution to heat capacity is due to chemical groups rather than atoms. Benson and coworkers³³ derived and analyzed groups from organic compounds with known heat capacity. Group value was calculated by the use of a least squares regression program. Table III is a compilation of the group value used to calculate constant-pressure heat capacities for liquids at 25°C and 1 atmosphere by Shaw²⁷. He observed that the precision of the application of the additivity rules in estimating heat capacity of liquids is ± 1.5 cal mole⁻¹ deg.⁻¹, and in most cases is better than ± 1 cal. mole.⁻¹ deg.⁻¹.

Indole, a heterocyclic compound, contains too many unknown groups to estimate the heat capacity by the additivity rules. However, one can borrow the principle of the additivity rules. If one assumes that the compound pyridine  to Pyrrole  is similar to the compound quinoline  to indole . The heat capacity difference between pyridine and pyrrole can be estimated by the difference between quinoline and indole. If the heat capacity of all but indole is known, the heat capacity of indole can be closely approximated as:

$$C_p(1)(\text{indole}) = C_p(1)(\text{Pyrrole}) + C_p(1)(\text{quinoline}) - C_p(1)(\text{pyridine})$$

where $C_p(1)(\text{pyrrole}) = 30.35 \text{ cal/mole, } ^\circ\text{C}^{29}$

$$C_p(1)(\text{quinoline}) = 47.6 \text{ cal/mole, } ^\circ\text{C}^{27}$$

$$C_p(1)(\text{pyridine}) = 32.04 \text{ cal/mole, } ^\circ\text{C}^{28}$$

then $C_p(1)(\text{indole}) = 45.91 \text{ cal/mole, } ^\circ\text{C}$

$$= 0.392 \text{ cal/g. } ^\circ\text{C.}$$

Table III

Group Values Used to Calculate Constant-Pressure Heat Capacity of Liquids at 25°C and 1 atm. Cal, mole⁻¹, deg.⁻¹.

Group	Value	Group	Value
Alkane		Olefin	
C-(C)(H) ₃	8.80	Cd-(H) ₂	5.2
C-(C) ₂ (H) ₂	7.26	Cd-(C)(H)	5.1
C-(C) ₃ (H)	5.00	Cd-(C) ₂	3.8
C-(C) ₄	1.76	Cd-(Cd)(H)	9.6
Aromatics		Cd-(Cd)(C)	7.9
C _B -(H)	5.3	C-(Cd) ₂ (H) ₂	14.3
C _B -(C)	2.9	C-(Cd)(C)(H) ₂	9.8
C-(C _B)(C)(H) ₂	6.3	C-(Cd)(C) ₂ (H)	9.4
Halogen		C _t -(C)	5.9
C-(Br)(C)(H) ₂	16.1	Cis-Corr	-1.3
C-(Cl) ₃ (C)	25.6	Rings	
Cd-(Cl) ₂	21.4	Cyclopentane	-4.8
C _B -F	8.6	Cyclopentens	-7.7
C _B -Cl	8.4	Cyclohexane	-6.5
C _B -Br	10.6	Cyclohexene	-8.7
Silicon		Cyclooctatetraene	-32.8
Si-(O)(C) ₃	0.0 (assigned)	Decaline	-13.1
O-(Si) ₂	21.6	Tetraline	-2.5
Oxygen		Sulfur	
O-(C)(H)	10.7	S-(C)(H)	12.5
O-(C) ₂	8.5	S-(C) ₂	10.7
O-(CO)(H)	13.6	S-(C _B)(H)	12.6
O-(CO)(C)	8.5	S-(S)(C)	9.2
O-(C _B) ₂	11.2	C-(S)(C)(H) ₂	5.8
CO-(O)(H)	10.0 (assigned)	C-(S)(C) ₂ (H)	3.7
CO-(O)(C)	7.0	C-(S)(C) ₃	2.9
CO-(C) ₂	12.6	C _B -(S)	0.0 (assigned)
C-(O)(C)(H) ₂	7.5	(CH ₂) ₃ - S	-2.5
C-(O)(C) ₂ (H)	8.8	(CH ₂) ₄ - S	-3.3
C-(O)(C) ₃	16.1 or 5.1	(CH ₂) ₅ - S	-5.1

Table III (cont'd)

$C-(O)(C_B)H_2$	12.0
$C_B - O$	0.0 (assigned)
Nitrogen	
$N-(N)(H)_2$	11.1
$N-(N)(C)_2$	10.5
$N-(N)(C)(H)$	7.6
$N-(C_B)(H)_2$	19.7
C_B-N	0.0 (assigned)
$Cd-(CN)(H)$	21.3
$O-(C)(NO_2)$	28.7

Appendix D

Method for the Estimation of the Latent Heat of Fusion

At the present time, there is no generally satisfactory method applicable for the estimation of the latent of fusion. A method suggested by Bauman³⁰, however, seems useful. He observed that the latent heat of fusion in calories per gram mole divided by the freezing temperature in °K is about 9 to 11 for organic compounds. Accordingly, the latent heat of fusion of indole is estimated to be approximately in the range of 25 to 30 cal/g. The following is a test of the Bauman estimation method for several materials for which the heat of fusion is known. The results are scattered indicating that great confidence can not be placed in the above results.

Organic Compound	Molecular Weight	M.P.		Heat of Fusion		$\Delta H_f / T_f$ °K
		°C	°K	cal/g	cal/mole	
Benzene	78.11	5.5	278.7	30.1	2348	8.42
Naphthalene	128.16	80	353.2	36.0	4608	13.05
Indene	116.16	-2	271.2	19.9	2312	8.52

SEPARATION AND PURIFICATION OF THE SOLID SOLUTION SYSTEM
INDOLE-INDENE BY CONTINUOUS COUNTERCURRENT COLUMNAR CRYSTALLIZATION

by

ALBERT TZE-HSUAN LIN

B.S. National Taiwan University, 1961

AN ABSTRACT OF A MASTER'S THESIS

submitted in partial fulfillment of the

requirements for the degree

MASTER OF SCIENCE

Department of Nuclear Engineering

KANSAS STATE UNIVERSITY
Manhattan, Kansas

1972

ABSTRACT

Two established mathematical models were introduced to test the experimental performance of the separation and purification of the solid solution indole-indene system by the continuous countercurrent columnar crystallization process. These models are the mass transfer limiting with latent heat effect model, by Meyer and Shen, and the mass transfer limiting model, by Gates.

Implicit in both of these models is the assumption that the purification crystallization process involves a simultaneous transfer of heat and mass between the countercurrent free liquid phase and solid phase streams. The mass transfer limiting with latent heat effect model is the result of the coupling of mass and energy continuity equations but it neglects interfacial mass transfer. While the mass transfer limiting model is simplified by considering only mass transfer effect.

The experimental concentration profiles obtained for indole-indene system operated under total reflux conditions were flat; the separations achieved in the crystallization column were small. The results showed that both of the models were applicable to the continuous columnar crystallization process for the solid solution indole-indene system. The measured effective axial diffusivities by the both models have values in the range 1.3 to 4.0 cm²/sec; literature data are ranged from low 0.5 to high 30 cm²/sec. The overall mass transfer coefficient calculated by the mass transfer limiting model has value $1.1 \times 10^{-3} \text{ sec}^{-1}$; literature data are ranged from low 0.13×10^{-3} to high $3.0 \times 10^{-3} \text{ sec}^{-1}$. These values are comparable with literature data.

The indication that a sharp change in concentration profile at the top of the crystallization column obtained for indole-indene system operated

under partial reflux condition is qualitatively in agreement with that of Meyer and Shen and Player, they studied the separation and purification of p-xylene -- m-xylene. Player assumed that this sharp change in concentration profile at the top of the crystallization column is due to the refreezing of the refluxed free liquid, which is a process associated with latent heat effect. This phenomena leads to the assumption by Player that the constancy of the solid and free liquid mass flow rates along the column would be inadequate.